# Effect of Tank Size on the Temperature Distributions for Hybrid Photovoltaic/Thermal Water Heaters

**Ahmad Al-Masri**

Submitted to the
Department of Mechanical Engineering
In partial fulfillment of the requirements for the degree of

Master of Science
in
Mechanical Engineering

Eastern Mediterranean University
September 2016
Gazimağusa, North Cyprus

Approval of the Institute of Graduate Studies and Research

Prof. Dr. Mustafa Tümer
Acting Director

I certify that this thesis satisfies the requirements as a thesis for the degree of Masters of Science in Mechanical Engineering.

Assoc. Prof. Dr. Hasan Hacişevki Chair,
Department of Mechanical Engineering

We certify that we have read this thesis and that in our opinion it is fully adequate in scope and quality as a thesis for the degree of Master of Science in Mechanical Engineering.

Prof. Dr. Uğur Atikol
Co-Supervisor

Asst. Prof. Dr. Murat Özdenefe
Supervisor

Examining Committee

1. Prof. Dr. Ibrahim Sezai _____
2. Assoc. Prof. Dr. Hasan Hacışevki _____
3. Asst. Prof. Dr. Murat Özdenefe _____

# ABSTRACT

In the present study an investigation was conducted on the temperature distribution effect for several tank capacities (100 L, 120 L, 150 L and 200 L) having two different aspect ratios (H/D) for each capacity. Hot water is supplied to these tanks by a Hybrid PV/T collector of 4 m² illuminating area. The circulation of water within PV cells cools its surface area to solve the problem occurred in PV cells, where each 1°C increase in the surface module 0.45% of the electrical efficiency decrease. A pump circulates water from the bottom of the tank to PV/T collector and then dropped it at the top of the tank in order to maintain thermal stratification. It was observed that tanks with a higher H/D ratio results a better performance, as hot water is stored in the tank at an earlier time (morning hours 6:00 until 9:00) than of tanks with a lower H/D ratios. It can be observed also that tanks with a higher H/D ratios, highly maintain thermal stratification occurred in the tanks than lower ratios. The tank for 100 L capacity having an H/D of 2.66 resulted the best performance at which stratification was highly maintained and the optimum tank is found to be for 150 L with an H/D of 2.97 as a larger capacity of domestic hot water is heated. The tank with 200 L tanks shall require a better insulation for conserving heat inside and prevent ambient losses.

**Keywords:** Hybrid PV/T collector, storage tanks, thermal stratification, aspect ratio.

# ÖZ

Bu çalışmada değişik tank kapasitelerinin (100 L, 120 L, 150 L ve 200 L) sıcaklık dağılımı iki değişik yükseklik-çap oranı (H/D) için araştırılmıştır. Sıcak su tanklara 4 m² ışıma alanı olan bir hibrit fotovoltaik-ısıl (PV/T) kollektör tarafından sağlanacaktır. PV/T düzeneğinde PV hücreleri içerisinde dolaşan su PV'nin yüzey alanlanını soğutarak her 1 °C lik sıcaklık artışının elektriksel verimde % 0.45 azalmaya sebep olması sorununu çözmeye yardımcı olmaktadır. Bu sistemde sıcak su tankında ısıl tabakalaşmayı sürdürmek için bir pompa tankın altından suyu alıp PV/T kollektörüne basıp tekrar tankın üzerinden geri döndürmektedir . Yüksek H/D oranı olan tankların ısıl tabakaylaşmayı daha iyi muhafaza ettikleri ve böylece daha iyi performans gösterdikleri gözlemlenmiştir. Isıl tabakalaşmanın muhafazasını eniyi H/D oranı 2.66 olan 100 L kapasiteli tank gösterirken, optimum değerler (daha fazla sıcak su depolanması) daha yüksek tank kapasiteli H/D oranı 2.97 olan150 L'lik tanktan alınmıştır. 200 L lik tankın ise daha iyi yalıtılması halinde depolanan ısıyı daha fazla muhafaza edebileceği ve ısıl kayıplarının azalacağı bulunmuştur.

**Anahtar kelimeler:** hibrit PV/T kollektör, depolama tankı, ısıl tabakalaşma, yükseklik-çap oranı

**To Allah almighty the most beneficent**

# ACKNOWLEDGMENT

I highly appreciate the guidance, recommendation and support given by my supervisor and mentor Assist. Prof. Dr. Murat Özdenefe and my co-supervisor Prof. Dr. Uğur Atikol. Infinitely I am grateful to my mother and her family for their support, help throughout my life and love. Even though I will never forget the pain of my father for his boundless faith in me, the inspiration of my dear brother and the sacrifices that he gave is beyond values. For this I would like to dedicate these long hours of work to God and to my family.

# TABLE OF CONTENTS

# LIST OF TABLES

# LIST OF FIGURES

# LIST OF SYMBOLS

| | |
|---|---|
| D | Diameter |
| DHW | Domestic Hot Water |
| H | Height |
| HWST | Hot Water Storage Tank |
| IDF | Input Data File |
| IPVTS | Integrated Photovoltaic Thermal System |
| PV | Photovoltaic |
| PVT | Photovoltaic Thermal |
| PV/T | Photovoltaic/Thermal |
| $q_{cond,n}$ | Conduction heat transfer between nodes |
| $q_{flow,n}$ | Heat transferred due to the flow of the fluid from the upper to lower node |
| $q_{invmix,n}$ | Inversion mix due to heat transfer from top to the bottom |
| $q_{oncycloss,n}$ | Heat losses to the environment during day time |
| $q_{offcycloss,n}$ | Heat losses to the environment during night time |
| $q_{source,n}$ | Heat transferred from the source side connection |
| $q_{use,n}$ | Heat transferred to the use side connection |
| T* | Temperature profile |
| TRNSYS | Transient System |
| WHST | Water Heater Stratified Tank |
| z | Node segment from bottom of the tank |

# Chapter 1

# INTRODUCTION

## 1.1 Background

The energy crisis facing the world today has left an open debate since the highest world energy demand belongs to fossil fuels which are polluting the earth [1]. Thus it is reasonable to evaluate a sustainable source of energy to minimize environmental impacts. The solar energy intercepted by earth surface reaches approximately to 900 W/m² in North Cyprus [2]. Thus in principle it is one of the most promising source of energy providing earth with heat and light.

Scientists and engineers developed an innovative sustainable energy technology such as the Hybrid Photovoltaic/Thermal (PV/T) system. However, Photovoltaic (PV) cells are generally temperature dependent and usually the efficiency of PV cells decreases about 0.45% for each degree rise in temperature [3]. The losses in the electrical energy generated due to the absorption of solar radiation are released as heat and the temperature of Silicon solar cells increases. Thus to remove the excessive heat from the module a fluid is circulated at the bottom surface of the non-illuminated area though copper pipes. The fluid absorbs heat and use it to fulfill thermal energy demands. The fluid can be either air or water, it is dependent on application service. This study concentrates on heating water as the working fluid. Furthermore, thermal energy storage is the main gap in this system due to insufficient amount of heat to cover thermal demands.

Thermal stratification process takes place in any water tank thereby stratification occurs due to mass differences of water, where less dense water with high temperature rises to the top of the water heater stratified tank (WHST) and cold water usually found to be at the bottom as shown in Figure 1.1. Water with low temperature react upon the gravity effect and flow to the bottom surface of the tank. The fluid is circulated and pumped from the bottom of the tank to the heat source which is the collector then dropped at the top surface of the tank. This flow maintain water stratification and is mainly considered in this work.

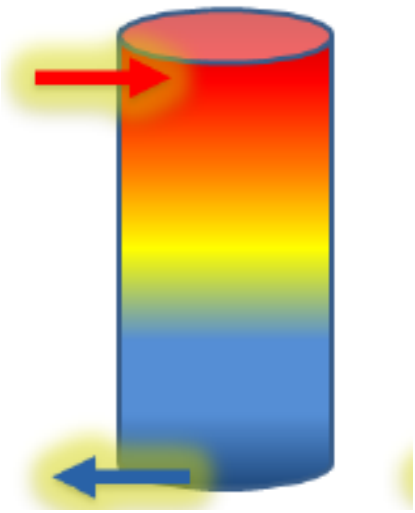

Figure 1.1: Thermal stratification effect.

The Hybrid Photovoltaic/Thermal (PVT) system has been widely investigated in the last decades. As it's been remarkable in the market PVT have achieved commercial success [2]. Therefore the generation of electricity and hot water by the same device has better chances of success than installing PV systems as it only generates electricity.

## 1.2 Aims and Objectives

This study aims to investigate the effect of temperature distribution inside several WHST sizes and capacities, under Cyprus weather conditions. The investigation focuses on the possibility of providing DHW with constant temperature during a day. The WHST height will be divided to several nodes. The thermal stratification is going to be investigated upon each node. This will enable us to have a better understanding of temperature distribution occurred in WHST to determine the optimum tank size for different usage patterns. Energy Plus software is utilized for running the simulation.

## 1.3 Thesis Organization

This dissertation is conveyed by seven chapters. In Chapter 2, a literature review was conducted where previous experiments on Hybrid PV/T systems in Cyprus and previous studies on temperature distributions in WHST.

In Chapter 3 the methodology is presented and the procedures of data collection and process analysis are displayed in detail.

The system modeling will be conducted in Chapter 4 for each of the components and the governing equations used by EnergyPlus.

In Chapter 5 the energy Plus simulation and the system topology will be explained in details.

In Chapter 6, the results and discussion of the investigation are displayed in details for different tank sizes, and finally in Chapter 7 the conclusion will be presented.

# Chapter 2

# LITERATURE REVIEW

## 2.1 Photovoltaic History

The PV effect was first observed by the French physicist Edmond Becquerel in 1839 [4]. He showed that certain material produces a small amounts of electric current when exposed to light. But it remained a curiosity of science until William Adams and Richard Day showed that light produce an electric current in Selenium. In the early of 1880's the first photovoltaic cells were built using selenium and gold leaf exhibiting 1%-2% efficiency [4]. Such a device was adopted in photography field for photometric devices. Selenium cells never become practical because of the highly cost comparing to their small efficiency. The most promising foundation was in the $19^{th}$ century by Charles Fritts, quantum mechanics laid the theoretical foundation for the present understanding of PV cells [4]. In 1950 a major step was developed for producing highly pure crystalline Silicon using a method called the Czochralsky method shown in Figure 2.1.

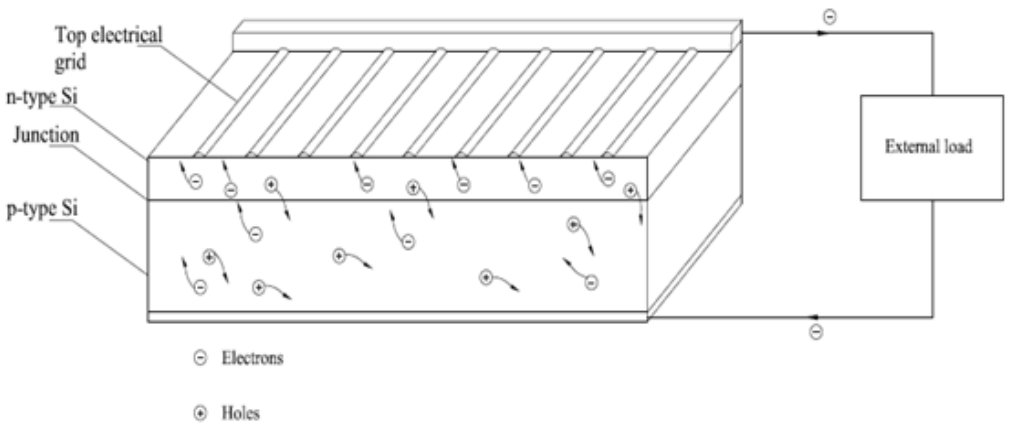


Figure 2.1: Czochralsky method PV cells, redrawn from Reference [4].

In 1954 Bell telephone laboratories developed PV cells to 6% efficiency and then to 11% heralding a new technology of solar electrical power generation. During the 20th century PV science was refined and increased efficiency to a maximum of 30% [4]. A Polycrystalline Silicon pc-S may achieve such efficiency under ideal conditions.

### 2.1.1 Physical aspect of solar cells efficiency

Typical PV cells efficiencies are about 10%-15% In the meanwhile engineers and scientists are working on lowering the cost of PV cells and enhancing its efficiency. Several aspects and physical conditions limit cells efficiency such as[4]:

- Low energy light that can't separate electrons from their bonds.
- High energy light beyond the needs to separate electrons from their bonds.
- Reflection and diffused radiation from PV cells surface.
- Resistance of current flow.
- High operating temperatures causing performance degradation of PV arrays.
- Self shading.

Usually untreated Silicon cells reflects 36% of solar radiation when it is intercepted, which in terms of efficiency is considered to be a horrendous loss [4]. Several ways are found to treat the cell surface using chemical coating and texturing the surface. Usually glazed glass lowers reflective beams to 5%. More often high temperature decreases the efficiency of solar PV cells. As agitated electrons starts to exceed the orbital and releases the energy thermally.

## 2.2 Hybrid PVT systems

Heat and electrical power can be simultaneously obtained by hybrid photovoltaic/thermal solar collectors. These systems consist of a PV array coupled with a working fluid circulated through copper pipes at the rear surface. Heat is being extracted from panel and transferred for domestic use.

The commercial PV module conversion efficiency is 6 to 15%. This output power may decrease by 0.2 to 0.5% per 1K increase in module temperature [5]. Thus, PV/T system is applied for heat recycling and temperature loss improving of PV module. The heat can be transferred to water or air depending on the application use such as bath, industrial preheat or air heating etc. These phenomena may adopt a higher energy conversion rate of the absorbed solar radiation. This system can be applied by natural or forced convection; it is dependent on the flow dynamic [5]. In Cyprus 93% of houses are based on solar water heaters to afford DHW [6].

An integrated photovoltaic and thermal solar system (IPVTS) was developed by Hung *et al.*2001[7] consisted of a PV/T module, storage tank, variable speed pump and controller. The daily average thermal efficiency of this system reaches approximately 0.38 and the daily overall efficiency is up to 0.50 [7]. A natural circulation PV/T system can reach a daily thermal efficiency of 0.4 and an overall efficiency of 0.55 [8]. The PV/T module technology can be classified for several types of applications such as air and water heating, refrigerant based and heat pipe based [9]. The thermosyphon water heating PV/T system can be applied with aluminum-alloy and/or copper flat box and the electrical efficiency reach 0.103 to 0.123 and the thermal efficiency range between 0.376 to 0.486, for summer and winter day [10].

A hybrid PV/T thermosyphon system was modeled for Nicosia, Cyprus conditions. to satisfy a family house of four persons [3]. The experiment was modeled for two types of glazed PV modules polycrystalline Silicon (pc-Si) and amorphous Silicon (a-Si). The PVT array is glazed and has an area of 4 $m^2$ coupled with a storage tank

of 120 L. The experimental results indicated an increase of total energy output of 532.1 kWh for pc-Si and 257.6 kWh for a-Si. However the electrical energy output was decreased by 38% comparing to total energy output of PV module. The system satisfies 50% of thermal energy needs supplied to the family [3].

The system shown in figure 2.2 was built with an illuminated area of 40 m² and 1500L storage tank. The fluid is driven by a pump. These systems were constructed and tested at the University of Patras [3] and simulated with TRNSYS program. It was shown that the overall energy production was increased which permits a higher chances of success for the hybrid system comparing to PV modules.

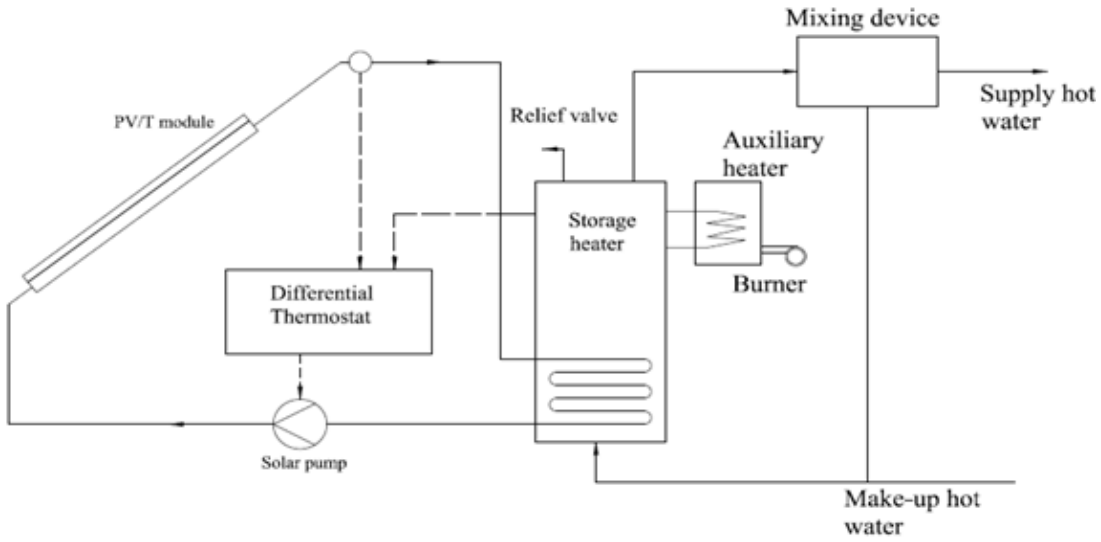


Figure 2.2: Hybrid PV/T schematic driven by solar pump redrawn from Ref. [3].

Another experiment was conducted by the University of Patras [11] studying the energy output to total solar radiation for a year where several modules tilted with same Latitude angle of 38.25°.Several aspects occurred for panels have different characteristics. Figure 2.3 helps to observe panel's aspects.

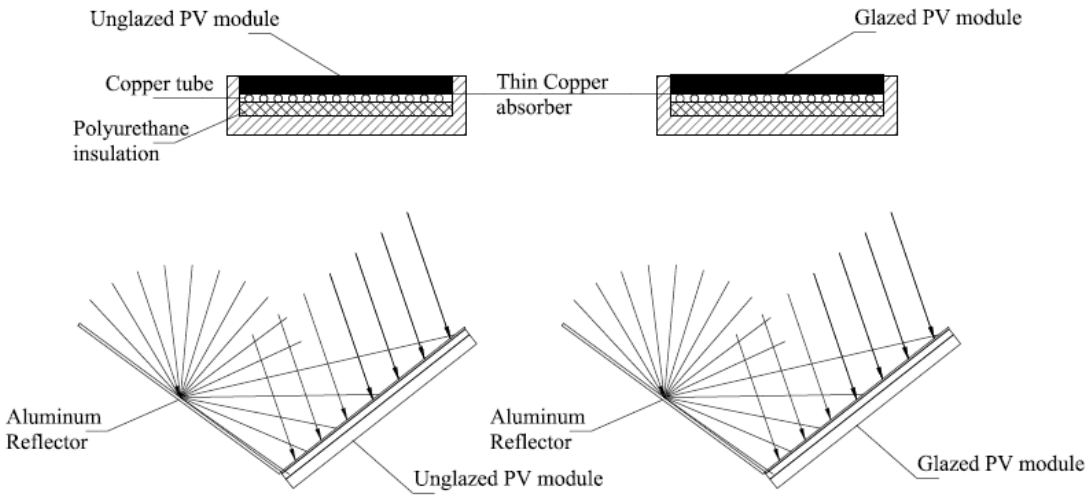


Figure 2.3: Four types of PV/T module including unglazed and glazed PV/T, unglazed module with reflector and glazed PV/T module with reflector. Ref. [11].

The operating temperature studied at 25°C, 35°C and 45°C in Cyprus. The experiment shows that PV/T systems with additional glazing has lower electrical total energy output of 165.92 kWh/m² for 25°C compared to unglazed PV/T and PV module. And it requires sufficiently higher thermal total energy output of 86255 kWh/m². It was shown that the use of a diffuse aluminum reflector between parallel rows of PV/T glazed module increases both energy. The electrical total energy output became of 186.63 kWh/m² and thermal total energy output 924.17 kWh/m² [11]. It is noted that the presence of the diffused reflector increased the thermal and electrical energy output. Both glazed and un-glazed PV/T module efficiency increased. The PV/T glazed plus reflector operates and results satisfactory solution to electrical and thermal energy needs. Therefore the system may afford environmental improvements.

## 2.3 Thermally stratified storage tanks

The main purpose of heat storage tanks in water heating system is to provide the sufficient quantity of DHW at a convenient temperature. This objective can be only

achieved if the stratification is maintained in the tank by preventing the mixing of cold and hot water, as hot water is being stored [12].

The degradation of thermal stratification in solar storage tanks are influenced by some factors, which it includes the conduction with the tank surface induced by natural convection, the heat loss to the environment, the mixing of cold and hot water and the diffusion of hot fluid which occurs within the tank [12].

The thermocline is a region of steep water temperature that separates and avoid the mixing of cold and hot water, thus the amount of DHW that can be extracted from the storage is dependent on the thickness of this region as figure 2.4 indicates, where the highly stratified storage tank has a smaller thermocline region thus conserving more hot water at the upper surface [12].

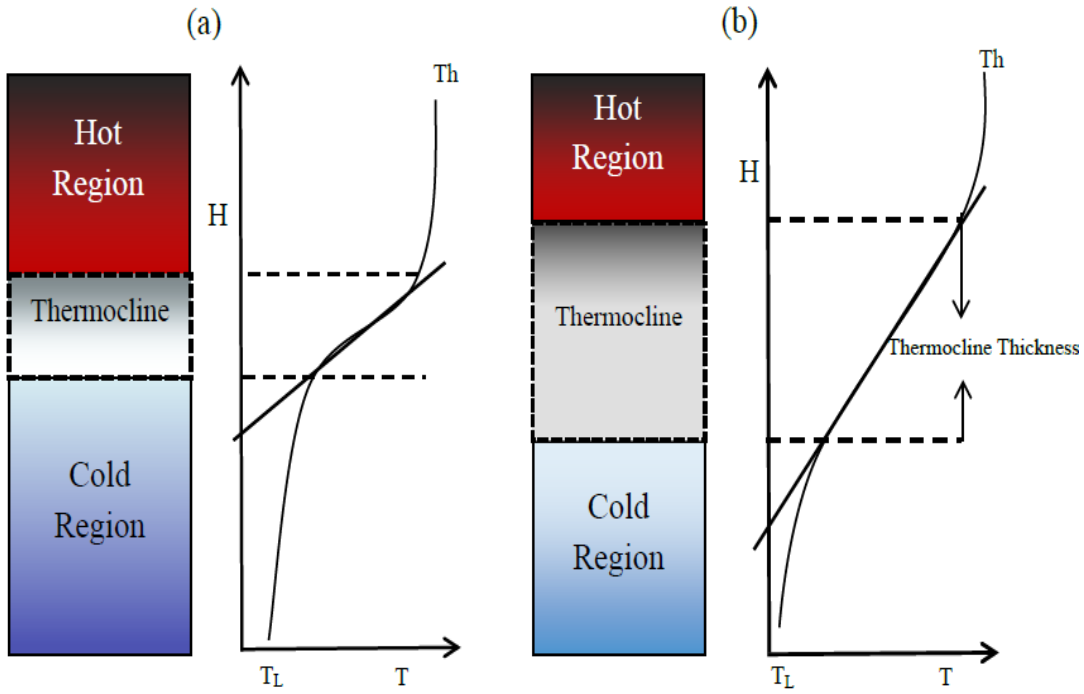


Figure 2.4 (a) Lower thermocline region for high stratification, (b) higher thermocline region for a moderately stratification.

Cynthia A.C and Stephen J.H [13]investigated the heat loss magnitude from a HWST designed for domestic applications. The rate of cooling of hot water was also tested during this experiment. The system is composed of an electric WHST of 270 L capacity, 1.50 m height and incorporated with a heat exchanger. In Figure 2.5 the schematic diagram is displayed as in reference [13]. It illustrates a temperature probe of nine nodes temperature levels, the distance between nodes is found to be 0.15m. The experimental values obtained were compared to that of computer simulations. Storage heat losses such as minimal wall conduction, temperature profile and uniform heat loss were also assumed in the computer simulation and investigated. Furthermore, it was determined that it is necessary to use heat loss parameters that accurately represent the thermal storage tank to adequately produce acceptable predictions [18].

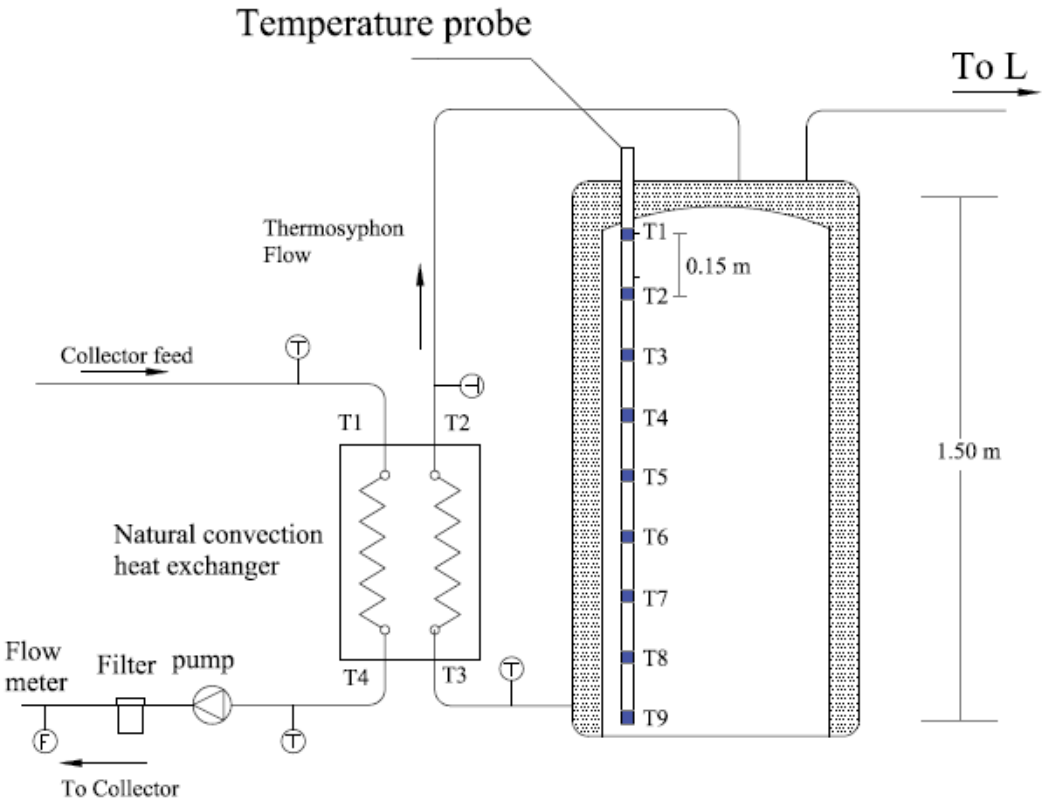


Figure 2.5: Schematic diagram illustrating the Vertical Temperature probe with 9 nodes, redrawn from Ref. [13].

Shyu, RJ., Lin, JY., Fang, LJ. at 1989 [14], conducted an experimental and theoretical study on the declining stratification in WHST. This study also discussed the effect of insulating the tank and thermal behavior on wall thickness of a stratified water tank. The tank wall axial conduction is one of the main factors which led to degradation in a stratified storage tank. Insulating the outside body of the tank prevent heat loss thus improving the performance. It was also observed that stratification can be highly maintained by insulating the inner wall of the tank. A model was developed which explains temperature distribution inside storage tanks, and the experiment verified the model by comparing results with numerical values [18].

An experimental investigation was conducted to determine the performance of solar horizontal HWST[15]. The efficiency of this system was investigated based on the extraction period and stranding time period of DHW by measuring the temperature distributions inside the tank. It was discovered that the thermal behavior of the storage tank is highly affected by the usage pattern of hot water [18]. Therefore, the usage of domestic hot water during summer period can be adequately met with the demand as for winter; the system has to interfere an auxiliary heater [9].

It was discovered that the cold water temperature entering the tank has a lower temperature than the one found at the bottom can improve the performance [16].The Eyecular industry provides Cypriot markets with water stratified tanks. In Figure 2.6 (a) and (b) the thermal stratification process occurring in the tank at heating mode and discharge mode is displayed to overview this process altering a lower thermocline region [17].

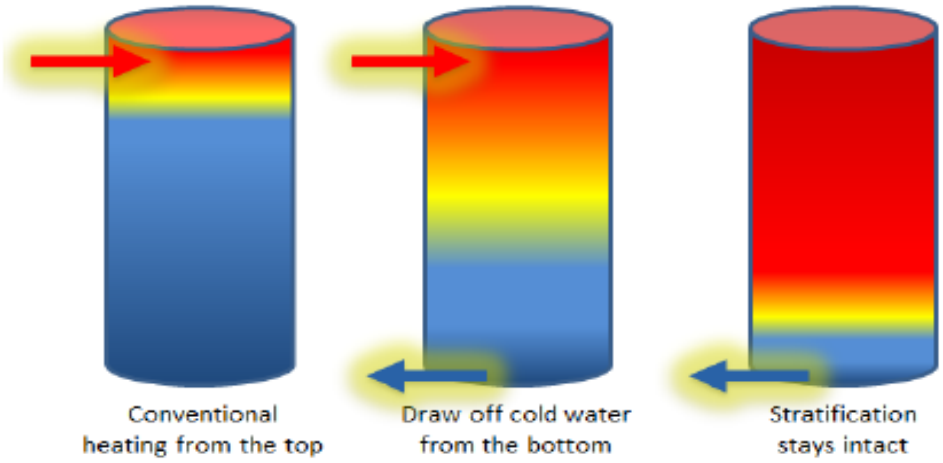


Figure 2.6 (a): Stratification is kept intact by heating from the top during heating mode [17].

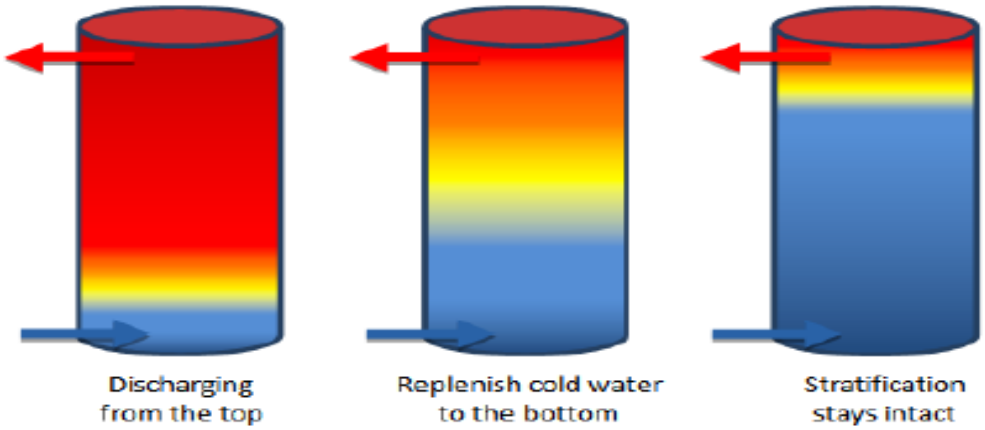


Figure 2.6 (b): Stratification is kept intact during discharge [17].

In this present study, the effect of the tank size on the temperature distribution will be investigated in consideration of different HWST capacities namely: 100L, 120L, 150L and 200L coupled with a hybrid PV/T module of 4m² illuminated areas. EnergyPlus simulation program will be used in this study.

# Chapter 3

# METHODOLOGY

## 3.1 Introduction

This study is conducted on a forced circulation of a Hybrid PV/T system as water is pumped to the collector from the bottom of the tank, which is known as integrated photovoltaic thermal system IPVTS. The investigation is based on different tank sizes with different capacities. The modeled water tanks are divided into 10 nodes of equal segments such as in Figure 3.1, assumed to be located in Cyprus. The system is simulated to investigate water thermal stratification occurring within the tanks. The storage tanks has different capacities; 100 L, 120 L, 150 L and 200 L. Three schemes will be considered to be simulated for each tank capacity shown in Figure 3.2. These schemes are generated based on varying diameter and/or height and hot water draw off periods. This may illustrate a better understanding of temperature distribution inside the WHST. It is important to notify that the auxiliary heater is disabled to assure that heating water is only based on solar energy collection. Thus, the schematic diagram is constructed only to investigate the effect of water thermal stratification produced from a Hybrid PV/T collector.

The hot water usage flow rate is calculated as in Turkish standards [19] which imply that one person consumes 50 L of warm water at 40°C. The extraction process time of DHW took 300 s at each draw off. Thus, the usage flow rate must be 0.16 L/s at the discharge point of the tank. This value is fixed for all fields, however in

EnergyPlus the extraction of water is considered to be for one hour at each draw off period.

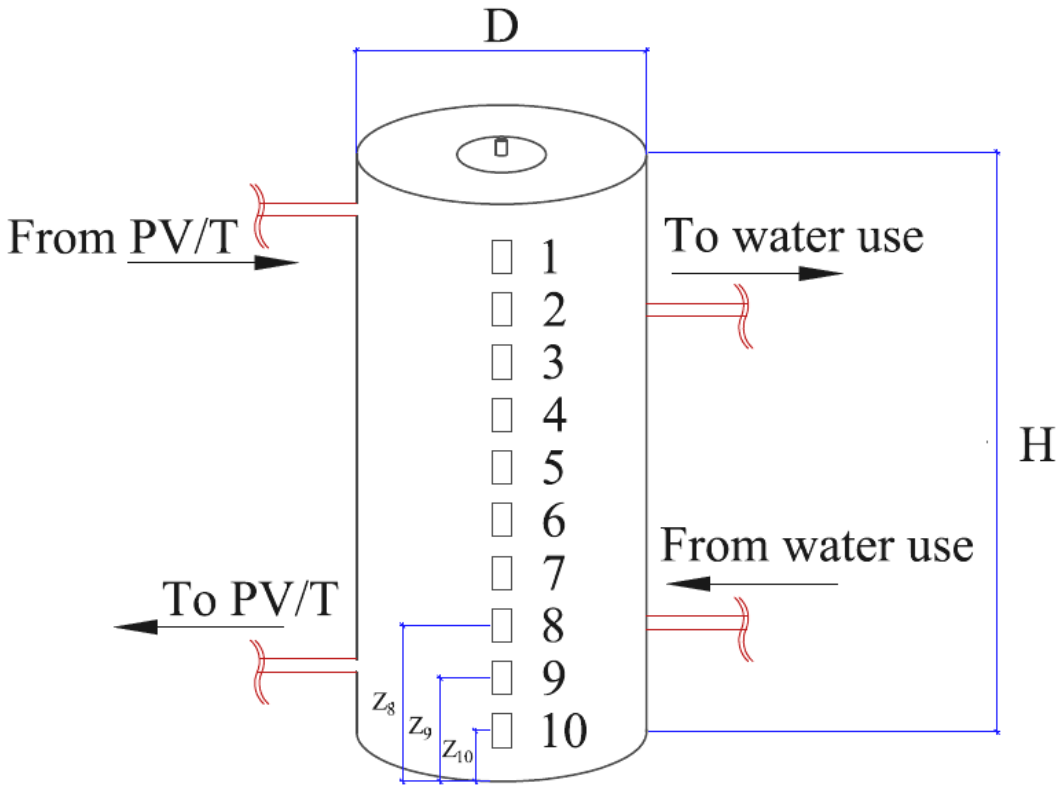


Figure 3.1: Water heater stratified tank (WHST) connection of supply and discharge pattern represented with 10 nodes, Height (H), Segment (Z) and diameter (D).

| | | Tank Capacity | | | | |
|---|---|---|---|---|---|---|
| Scheme | Parameter | 100 L | 120 L | 150 L | 200 L | |
| Scheme1 | H/D | 2.07 | 1.81 | 2.22 | 2.29 |  |
| | Draw Off time | 1- 9:00 - 10:00<br>2- 13:00 - 14:00 | 1- 9:00 - 10:00<br>2- 13:00 - 14:00 | 1- 9:00 - 10:00<br>2- 13:00 - 14:00 | 1- 9:00 - 10:00<br>2- 13:00 - 14:00 | |
| Scheme 2a | H/D | 2.66 | 2.40 | 2.97 | 3.92 |  |
| | Draw Off time | 1- 9:00 - 10:00<br>2- 13:00 - 14:00 | 1- 9:00 - 10:00<br>2- 13:00 - 14:00 | 1- 9:00 - 10:00<br>2- 13:00 - 14:00 | 1- 9:00 - 10:00<br>2- 13:00 - 14:00 | |
| Scheme 2b | Draw Off time | 1- 18:00 - 19:00 | 1- 18:00 - 19:00 | 1- 18:00 - 19:00 | 1- 18:00 - 19:00 | |

Figure 3.2: Schemes parameters.

## 3.2 Tank size and capacity

A water storage tank is a cylinder which stores hot water for domestic use having a capacity volume and size (height and diameter). A tank with 100 L capacity has the same volume with different height for different diameter and vice versa. Thus, the tank might experience different stratification process for different height and diameter. The aspect ratio of a storage tank is the ratio of height (H) to diameter (D) and there is no specific guideline specifying the maximum height to diameter ratio, not even in American Petroleum Institute manuals. For that three schemes are generated in this study at which each of the scheme require different parameters by varying H or D or time of extracting hot water, this may afford better understanding about thermal stratification occurred in Storage tanks. It should be noted while generating schemes the Diameter is always assumed but the height is being calculated using the volume formula of a cylinder for each tank volume (100 L, 120 L, 150 L and 200 L).

### 3.2.1 Scheme 1

In this scheme water tanks are simulated to have a variable diameter with the same height approximately as shown in Figure 3.2. In this scheme there are two draw off periods which the first one starts at 9:00 and ends at 10:00 and the second draw off starts at 13:00 and ends at 14:00 as displayed in Figure 3.3. Three hours are considered to be the standing time period between two draw offs for heating recovery.

### 3.2.2 Scheme 2

In this scheme the water tanks are modeled to have a variable heightfor each tank volume as for the Diameter is taken to be constant for 0.40 m. is divided into two sections named scheme 2a and scheme 2b as shown in Figure 3.2. At which scheme

2a state that the tank draws off periods are same as scheme 1 as shown in Figure 3.3. The results of this scheme are compared with scheme 1 giving an understanding about the effect of tank sizes (diameter and height) difference to select an appropriate tank.

In scheme 2b the extraction of hot water starts at the end of the day from 18:00 and ends at 19:00. Thus, the collector is heating water though all day hours without any usage of DHW. This scheme helps us to understand the stratification effect in the water tank for a full heating day and an extraction of DHW during night time. The results of this scheme are compared only with scheme 2a.

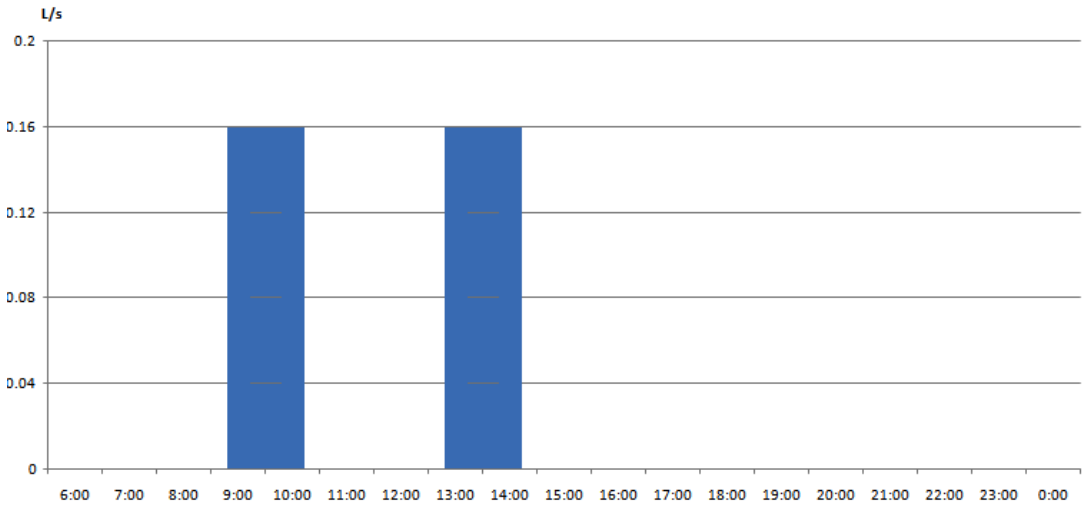

Figure 3.3: Volumetric flow rate extraction per day for scheme 1 & 2a.

## 3.3 Simulation process

The methodology process adopted in this study is illustrated in Figure 3.4. Whenever solar radiation is available, heat is extracted from the collector; water is being heated and supplied to tank. The graphical analysis of hot water inside the tank is displayed by dimensionless height z/H and dimensionless temperature $T^*$. The temperature profile is followed by the formula below:

$$T^* = \frac{T(z,t) - T_{min}}{T_{max} - T_{min}} \quad (3.1)$$

where:

$T_{min}$ = Minimum water temperature

$T_{max}$ = Maximum temperature

$T(z, t)$ = Temperature of hot water for height z and time t

H represents the height of the tank and z is the segment from the bottom of the tank to node level. The graph enables us to analyze the effect of thermal stratification occurring in each of the tanks represented in the schemes. $T(z,t)$represents the hot water temperature in each node at a particular time as obtained in simulation. While $T_{max}$ is hot water maximum temperature during draw off at discharge. $T_{min}$ is the minimum temperature supplied to the tank.

During day time and during discharge time for scheme 1 and scheme 2a, hot water is supplied to the tank at a flow rate of 0.16 L/s to maintain equilibrium inside the tank. Thus, during draw off periods HW is not fully discharged from the tank in consequence of water is supplied to the tank at the same flow rate.

The ambient temperature for Cyprus and solar intensity are measured in EnergyPlus program. Figure 3.5 shows the solar radiation and environmental temperature per day, where the total solar radiation on the horizontal surface H is obtained by Energy Plus simulation as for the total solar radiation on tilted surface and the beam radiation on tilted surface are calculated by excel sheet using the formula below [26].

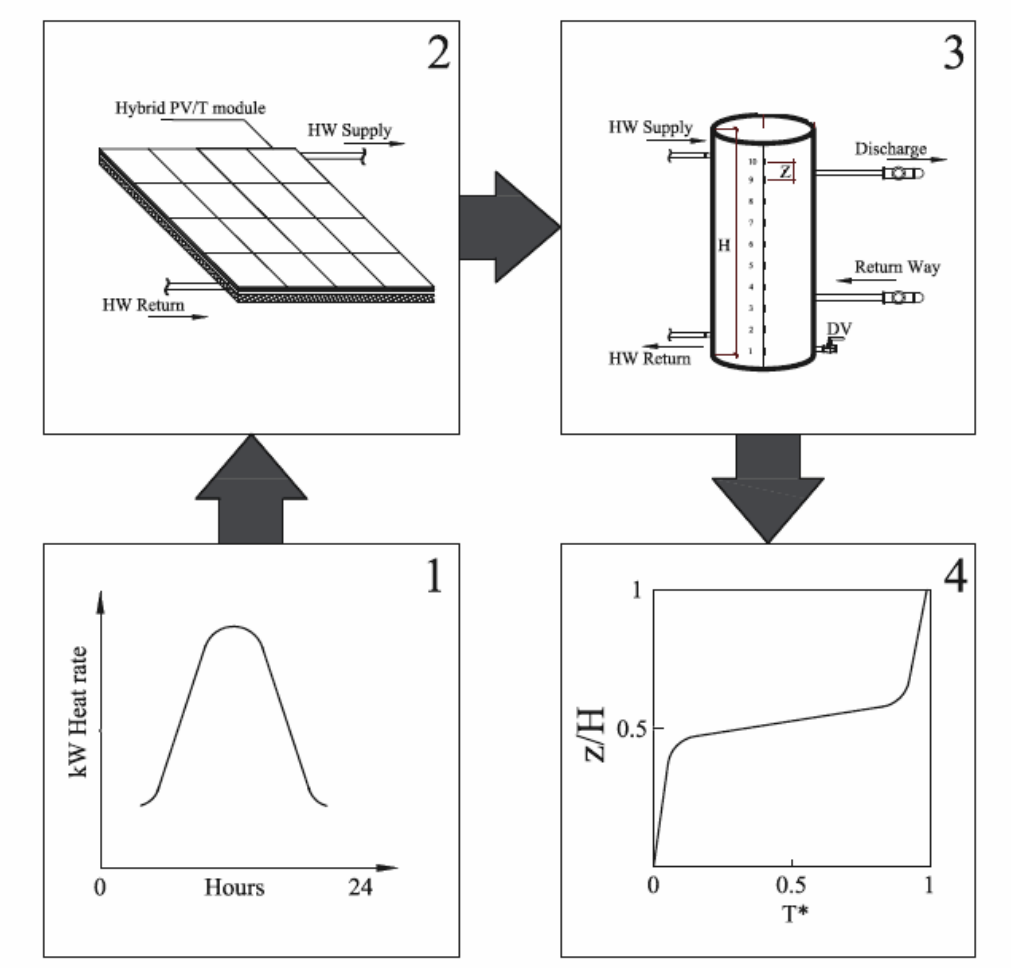


Figure 3.4: The methodology diagram.

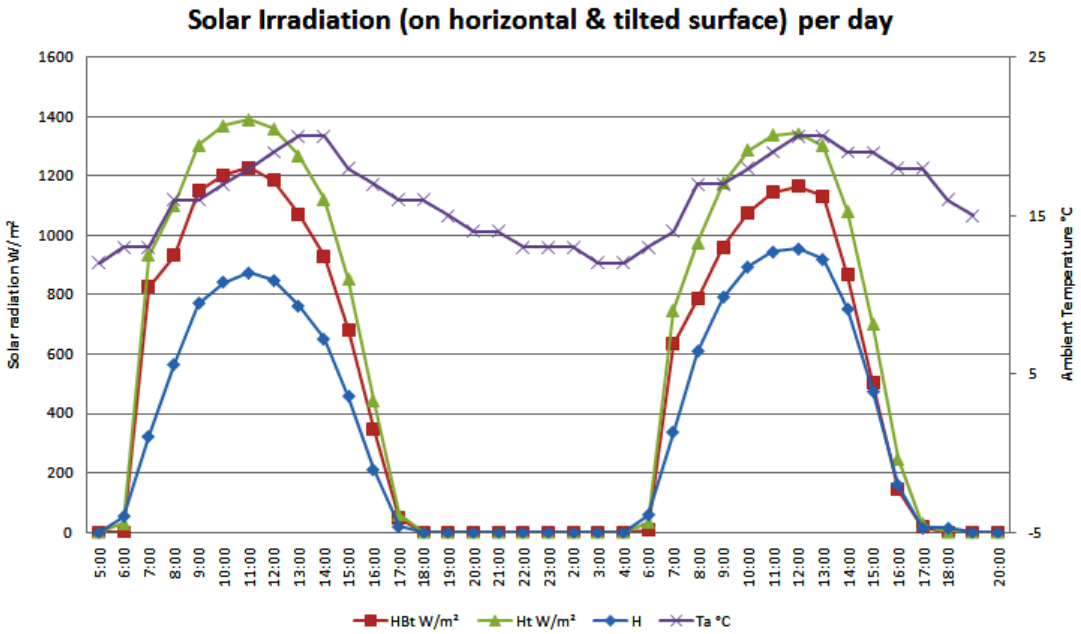


Figure 3.5: Solar intensity and ambient temperature obtained for February 21-20 provided for Larnaca in EnergyPlus.

The solar radiation on the horizontal surface is obtained by EnergyPlus, The tilted solar radiation and beam tilted solar radiation is calculated based on the following equations. The earth angle of declination is given by [26]:

$$\delta = 23.45\, Sin[\left(\frac{360}{365}\right)(284 + n)] \tag{3.2}$$

where:

δ = Angle of declination

n = Number of the day which is 51 and 52

The altitude angle and the incident angle are calculated by the following equations

$$Sin\,(\alpha) = Cos\,(z) = Sin\,(L)Sin(\delta) + Cos\,(L)Cos(\delta)\,Cos\,(h) \tag{3.3}$$

$$Sin\,(i) = Cos\,(L - S)Cos(\delta)\,Cos\,(h) + Sin\,(L - S)Sin(\delta) \tag{3.4}$$

where:

α = Altitude angle of the sun

z = Zenith angle of the sun

i = The incident angle of solar radiation

L = Latitude angle of Cyprus (35.12°)

S = Tilted surface angle of PVT collector (30°)

h = Solar hour angle which is ± ¼ minutes from 12:00 pm.

The beam radiation at normal incidence is given by calculating constant for a selected month. The beam radiation incident on a horizontal surface and diffused sky radiation are given to calculate the total solar radiation on a horizontal surface [26].

$$H_{Bn} = Ae^{-\frac{B}{Sin}}(\alpha) \quad (3.5)$$

$$H_B = H_{Bn} Sin\,(\alpha) \quad (3.6)$$

$$H_d = CH_{Bn}F_{SS} \quad (3.7)$$

$$H = H_B + H_d \quad (3.8)$$

where:

$H_{Bn}$ = The beam radiation at normal incidence

A = Apparent solar radiation for February (1214.52 W/hr.m²)

B = Atmospheric extinction coefficient (0.144 for February)

$H_B$ = beam radiation incident on a horizontal surface

$H_d$ = Diffused sky radiation

C = Diffused radiation factor which is 0.06 for February

$F_{SS}$ = Angle factor between surface and sky which is 0.5

H = Total solar radiation on a horizontal surface (given by EnergyPlus)

The total radiation tilt factor $R$ and beam radiation tilt factor $R_B$ are calculated to achieve the amount of solar radiation on a tilted surface which are given by the following equations:

$$R_B = \frac{Cos\,(i)}{Cos\,(z)} \quad (3.9)$$

$$R = \left(\frac{H_B}{H}\right) R_B + \left(\frac{H_d}{H}\right)\left[\frac{1 + Cos(s)}{2}\right] + \rho_g \left[\frac{1 - Cos(s)}{2}\right] \quad (3.10)$$

where:

$\rho_g$ = Surface snow constant which is 0.22 for a surface without snow

Finally the tilted beam radiation and total radiation on tilted surface are calculated by the following equations:

$$H_{Bt} = R_B H_B \tag{3.11}$$

$$H_t = HR \tag{3.12}$$

where:

$H_{Bt}$ = The beam radiation on a tilted surface

$H_t$ = The total solar radiation on a tilted surface

# Chapter 4

# SYSTEM MODELING

## 4.1 Schematic diagram

The Integrated Photovoltaic Thermal System schematic diagram investigated in this study is shown in Figure 4.1. This system is consisted of a PV/T collector, a WHST, variable speed pump and a controller setpoint [7]. The governing equations for each component are going to be explained in this chapter. The equations presented in this chapter are acquired from engineering reference guide of EnergyPlus [23].

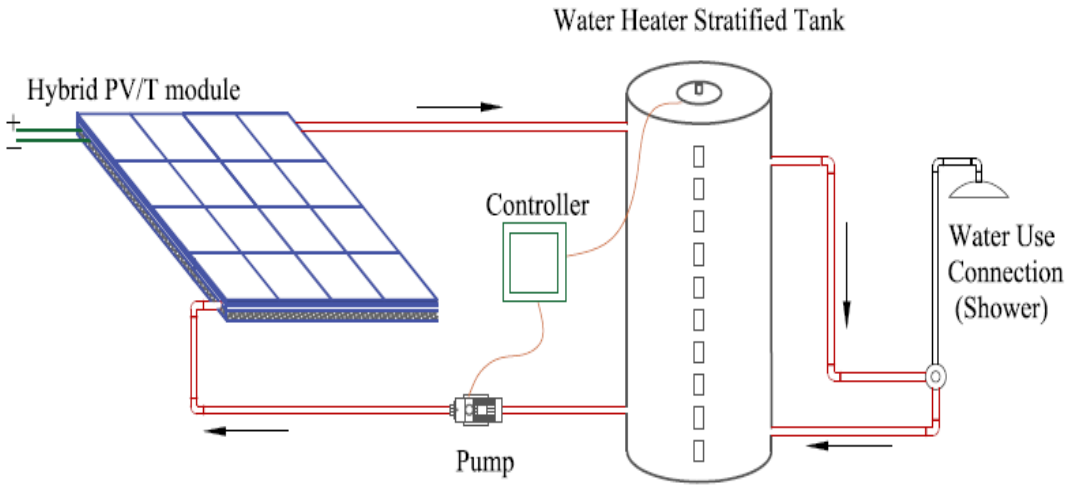


Figure 4.1: Schematic of an IPVTS.

## 4.2 The Hybrid PV/T system modeling

The unglazed PV/T module investigated for this study has the following characteristics which are given in Table 1. Using these parameters the PV/T is going to be modeled with EnergyPlus. For an area of 4 m² several sizes of WHST is going

to be investigated. In Figure 4.2 the module is specified describing the composition of the module as well pipe connection.

Table 4.1: Characteristics of the solar Hybrid PV/T collector considered

| Parameter | Characteristics |
|---|---|
| Area of the collector | 4 m² |
| Absorber plate thickness | 0.5 mm |
| PV module | Poly-crystalline Silicon (pc-Si) |
| Copper pipe diameter | 1.875 cm |
| Fiberglass Insulation thickness | 50 mm |

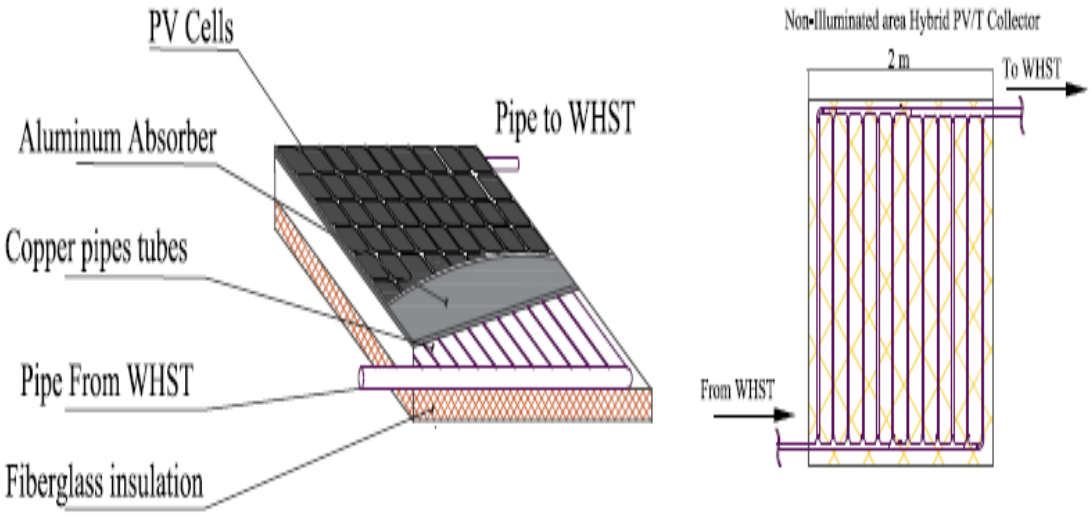


Figure 4.2: Hybrid PV/T module materials formation and connections.

The EnergyPlus "Solarcollector:FlatPlate:PhotovoltaicThermal" object is a simple PV/T model for quick design study [23]. Details input data are required for the construction of the PVT collector. This model found on EnergyPlus is heating either air or liquid as a working fluid. In this study PV/T system is heating water as the working fluid. When PV/Thermal collector is controlled to be "on", the model is able

to calculate the temperature at the outlet pipe of the PV/T collector using the following equations. The surface fraction with the PV/T collector ($f_a$) is the area of the collector that is active. The surface area of the PV/T will be multiplied by 0.9 at which only 90% of the module is active cells. This number is divided by the gross area of the surface where the module is located and the gross area should includes no windows.

$$Q_{collct} = A_a \, f_a \, G_T \, \eta_{thermal} \tag{4.1}$$

$$f_a = 0.9 \, {}^{A_a}/_{A_G} \tag{4.1}$$

where:

$Q_{collect}$ = Heat collected, [W]

$A_a$ = Net surface area of the collector [4 m²]

$G_T$= Solar radiation on PV/T collector [W/m²]

$f_a$= The active surface fraction with the PV/T collector

$A_G$= The gross area of the roof surface, including no windows [9 m²]

The outlet temperature of the PV/T collector is given by:

$$T_{out} = T_{in} + \frac{Q_{collect}}{\dot{m} C_p} \tag{4.2}$$

where:

$T_{out}$ = The outlet temperature node of the PV/T, [°C]

$T_{in}$ = The inlet temperature node of the PV/T, [°C]

$\dot{m}$ = The mass flow rate of water through the PV/T, [kg/s]

$C_p$ = The specific heat of water, [J/kg.°C]

The electrical power an electrical efficiency is determined under operating conditions. There are four parameters in the model which cannot be determined by physical measurements which are $I_{L,ref}$ , $I_{O,ref}$ , g and $R_S$ [25].The Energy Plus model calculates those values from manufacturers catalog data.

$$I = I_L - I_o e^{[\left(\frac{q}{v.K.T_c}\right)-1]} \tag{4.3}$$

$$I_L = I_{L,ref} \frac{G_T}{g} \tag{4.4}$$

$$I_O = \left(\frac{T_c}{T_{c,ref}}\right)^3 . I_{O,ref} \tag{4.5}$$

$$T_c = T_{amb} + \left(\frac{1 - \frac{\eta_c}{\tau\alpha}}{G_T \, {\tau\alpha}/{U_L}}\right) \tag{4.6}$$

$$\mathrm{v} = A_C N_S \tag{4.6}$$

$$P = A_C f_a G_T \eta_c \eta_{invert} \tag{4.7}$$

$$V = P/I \tag{4.8}$$

where:

I = Current flow generated [A]

$I_L$= Module Photocurrent [A]

$I_O$ = Diode reverse saturation current [A]

q = Electron charge constant [1.602176565×10−19, C]

$\nu$ = Empirical PV curve fitting parameter

K = Boltzmann constant [J/K]

$T_C$ = Temperature of the collector [K]

$I_{L,ref}$ = Module Photocurrent at reference condition [A]

g = solar intensity taken [1000 W/m²]

$T_{C,ref}$ = Temperature of the collector at reference condition [K]

$I_{O,ref}$ = Diode reverse saturation current at reference condition [A]

$\eta_c$ = Efficiency of the collector

$\tau\alpha$ = Transmission and absorption coefficient

$A_c$ = Area of the collector [m²]

$N_s$ = Number of module in series

$P_{elec}$ = Electrical Power generated [W]

$\eta_{inver}$ = DC to AC conversion efficiency [0.9]

V = Load voltage [V]

The simulation process of a PVT collector, have flow rate for the circulatingwater that ranges between 0.12 L/s to 0.16 L/s, some inputs can be auto-sizable.

The steady state efficiency is calculated:

$$\eta_{thermal} = \dot{m}C_p(T_{out} - T_{in})/(GA_a) \quad (4.9)$$

The electrical efficiency equation is given by:

$$\eta_{electrical} = P_{elec}/(GA_a) \quad (4.10)$$

The overall efficiency is given by:

$$\eta_0 = \eta_{electrical} + \eta_{thermal} \quad (4.11)$$

## 4.3 Water Heater Stratified Tank modeling

The object "WaterHeater:Stratified" in EnergyPlus is modeled by dividing the WHST into 10 nodes. The differential equation governing the energy balance which is solved numerically by the Euler method is:

$$m_n C_p \frac{dT_n}{dt} = q_{net,n} \quad (4.12)$$

where:

$m_n$ = the mass of water at node n

$C_p$ = Water specific heat

$T_n$ = Temperature at n node

t = time

$q_{net,n}$ = heat transfer rate at node, n

It is necessary to notify here that the $q_{net,n}$ is the summation of multiple heat transfer due to losses and gains. The given equation is:

$$q_{net,n} = q_{oncycloss,n} + q_{offcycloss,n} + q_{cond,n} + q_{use,n} + q_{source,n} + q_{flow,n} + q_{invmix,n} \quad (4.13)$$

where:

$q_{oncycloss,n}$ = Heat losses to the environment

$q_{offcycloss,n}$ = Heat losses from the ambient to the tank

$q_{cond,n}$ = Conduction heat transfer between upper and lower nodes

$q_{use,n}$ = Heat transferred to the use side connection

$q_{source,n}$ = Heat transferred from the source side connection

$q_{flow,n}$ = Heat transferred due to the flow of the fluid from the upper to lower nodes

$q_{invmix,n}$ = Inversion mix due to heat transfer from top to the bottom of the tank

The$q_{oncycloss,n}$ and $q_{offcycloss,n}$ are define as:

$$q_{oncycloss,n} = \left(UA_{tank} + UA_{add,n}\right).(T_a - T_n) \quad (4.14)$$

$$q_{offcycloss,n} = \left(UA_{tank} + UA_{flue}\right).(T_a - T_n) \quad (4.15)$$

where:

$UA_{tank}$ = loss coefficient of the tank to the environment

$UA_{add,n}$ = Node loss coefficient added to the tank

$UA_{flue}$ = loss coefficient to the environment

$T_a$ = Ambient temperature

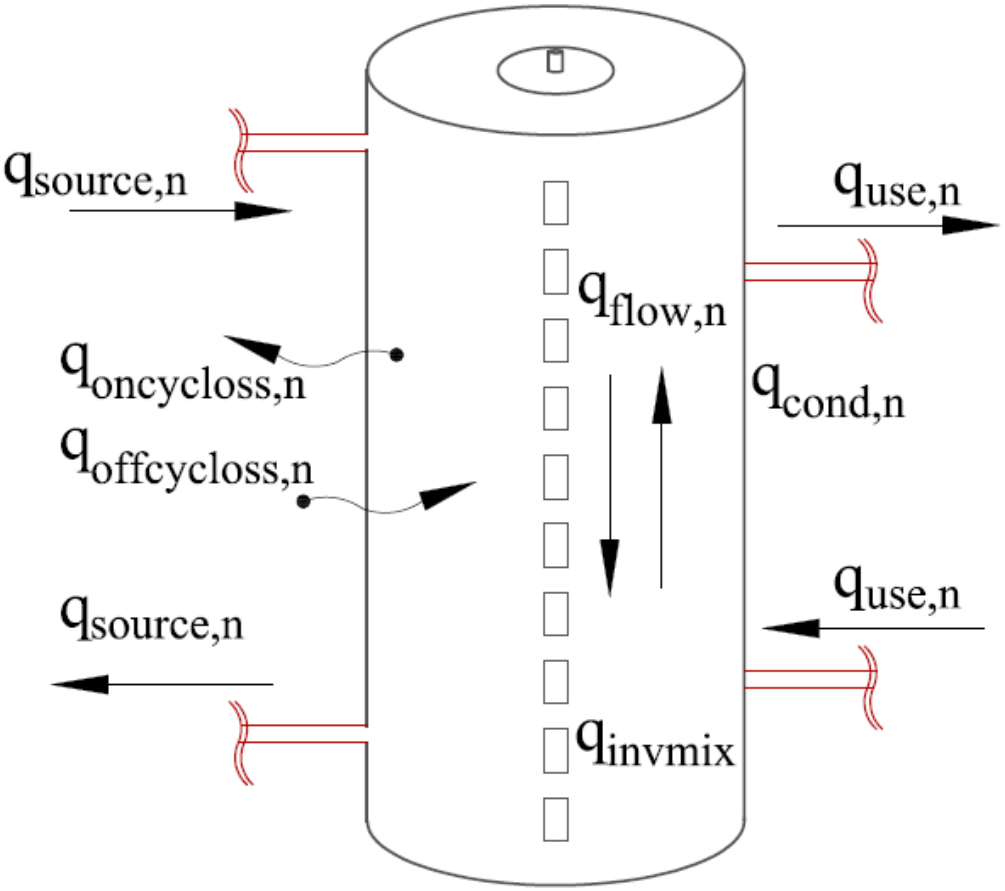


Figure 4.3: Energy balance occurring the WHST.

The $q_{cond,n}$ governing equation is:

$$q_{cond,n} = \frac{KA_{n+1}}{L_{n+1}}(T_{n+1} - T_n) + \frac{KA_{n-1}}{L_{n-1}}(T_{n-1} - T_n) \tag{4.16}$$

where:

K = Water thermal conductivity

$A_{n+1}$ = Surface area shared from n to n+1

$L_{n+1}$ = Length from the center of mass of n to n+1

$T_{n+1}$= Temperature of n+1

$A_{n-1}$= Surface area shared from n to n-1

$L_{n-1}$= Length from the center of mass of n to n-1

$T_{n-1}$= Temperature of n-1

The$q_{use,n}$ and $q_{source,n}$ equation are defined as

$$q_{use,n} = \varepsilon_{use}\, \dot{m}_{use}\, C_p (T_{use} - T) \tag{4.17}$$

$$q_{source,n} = \varepsilon_{source}\, \dot{m}_{source}\, C_p (T_{source} - T) \tag{4.18}$$

where:

$\varepsilon_{use}$ = The effectiveness of heat exchanging for use-side connections

$\dot{m}_{use}$ = Use-side mass flow rate

$T_{use}$ = use-side inlet temperature

$\varepsilon_{source}$ = The effectiveness of heat exchanging for source-side connections

$\dot{m}_{source}$ = source-side mass flow rate

$T_{source}$ = Source-side inlet temperature

The$q_{flow,n}$ defined as:

$$q_{flow,n} = \dot{m}_{n+1} C_p (T_{n+1} - T_n) + \dot{m}_{n-1} C_p (T_{n-1} - T_n) \tag{4.19}$$

where:

$\dot{m}_{n+1}$= n+1, node mass flow rate

$\dot{m}_{n-1}$= n-1, node mass flow rate

The inversion mixing process occurs very rapidly when the node at the bottom surface of the tank is warmer than the above surface. The temperature difference drives a difference in density that cause mixing.

$$q_{invmix\ ,n} = \dot{m}_{invmix\ ,n+1} C_p \left(T_{invmix\ ,n+1} - T_n\right) + \dot{m}_{invmix\ ,n-1} C_p \left(T_{invmix\ ,n-1} - T_n\right) \quad (4.20)$$

The $q_{invmix\ ,n}$ is the maximum value of the node mass and substep which will afford a stability to the solution given:

$$\dot{m}_{\text{invmix ,n}} = 0.5\ {}^{\dot{m}_n}/_{\Delta t} \quad (4.21)$$

The EnergyPlus modeling incorporates all these equations into the original differential equation and solves it. The outlet source temperature and inlet use temperature is found by the equation below if the effectiveness value is less than 1.0, the equation are defined as follows:

$$T_{use\ out\ ,n} = T_{use\ ,n} + \frac{q_{use\ ,n}}{\dot{m}_{use}\, C_p} \quad (4.22)$$

$$T_{source\ \ out\ ,n} = T_{source\ ,n} + \frac{q_{source\ ,n}}{\dot{m}_{source}\, C_p} \quad (4.23)$$

where:

$T_{use\ out\ ,n}$ = Use side outlet temperature

$T_{source\ \ out\ ,n}$ = Source side outlet temperature

All node temperatures for $q_{net\ ,n}$ are considered to be old from the previous substep. At a given node the new temperature is calculated by the equation below:

$$T_n = T_{n,old} + \frac{q_{net,n}\Delta t}{m_n C_p} \quad (4.24)$$

## 4.4 Controller Setpoint manager

The controller object is modeled by defining schedules on EnergyPlus. The Schedules are to be shown in chapter 5. Schedules alter no general equations managing time with inputs is the main application. The basic concept of this component is to control fluid flow through the solar collector based on the two temperature inputs principles. Schedules tend to manage timing of work using on and off period and managing schedules for PVT electrical and thermal efficiency.

## 4.5 Variable speed pumps

A pump with variable named "Pump:VariableSpeed" object which in turns operate the physical limits of the device by defining the flow rates at a maximum of 0.3 L/s and minimum of 0 L/s (at night time). This pump will select a flow rate between the maximum and minimum limits and try to meet the flow request by demand side components. This pump is intermittent and active only when solar radiation is intercepted by the collector.

The Total efficiency of the pump is given by:

$$\eta_P = {}^{\eta_T}/_{Motor\ Efficiency} \quad (4.25)$$

## 4.6 Water use equipment

Water system for demand side is modeled as an essential part of the water system where water is being utilized for a purpose. The "water use" modeling is accomplished by two input objects which are the "water use equipment" and "water

use connection". This equipment simulate different type of water usage and for this study a shower is considered to be the usage equipment. Water use equipment is not connected directly to the plant but it is connected to water use connection which is connected to the WHST.

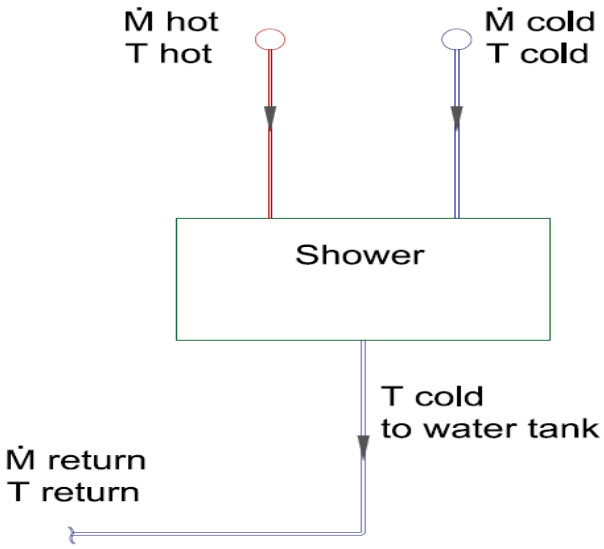

Figure 4.4: Water use connection subsystem

The water use connection object manages the equipment by solving the subsystem shown in figure 4.4. The heating rate and energy by the following equation:

$$\boldsymbol{Q} = \dot{m}.\boldsymbol{C_p}(\boldsymbol{T_{hot}} - \boldsymbol{T_{return}}) \tag{4.26}$$

where:

Q =heating rate

$C_p$= Specific heat water (4.187 kJ/kg.K)

$T_{hot}$= Temperature of water supplied to shower

$T_{return}$ = Temperature of water returned to the tank

# Chapter 5

# ENERGY PLUS AND SYSTEM TOPOLOGY

## 5.1 Overview of Energy Plus

The simulation is conducted on the basis of EnergyPlus V8.5 program which is a load simulation and energy analysis program, the US Department of Energy developed this program[21]. The use of this program is validated [25]. In order to run the simulation successfully with EnergyPlus, it is necessary to understand the working principles of all the components of the system, and to introduce the system by means of input file to Energy Plus.

### 5.1.1 Energy Plus EP-Launch

The EP-Launch is a component of Energy Plus that enables users to open text editor for input files, drawing files, output files and weather data file. The weather data file is a file which includes values for the environmental parameters such as environmental temperature, solar radiation, wind speed etc. In Figure 5.1 a screenshot shown to display the EP-Launch window showing the uploaded weather Data file. The “Edit-IDF Editor” will access to a window where all the input parameters for the simulation is entered. The “Simulate” button starts the simulation process when all data are uploaded and when IDF file is completely constructed.

### 5.1.2 Energy Plus Input Data File (IDF) Editor

Energy Plus models are formatted by the standard IDF file used for editing and entering the input data. This file contains necessary data for the description of

modeling system. The IDF is a text file but with an extension of '.idf' instead of '.txt'[22].

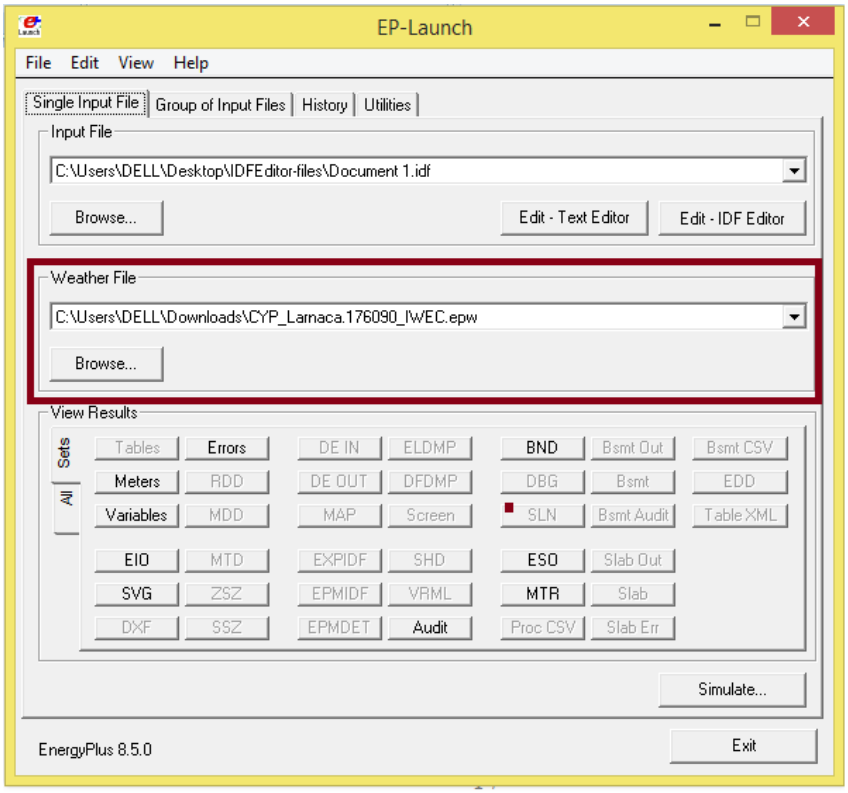

Figure 5.1: EP-Launch screen.

### 5.1.3 Plants in Energy Plus

A strategy must be interpreted to model a system on the IDF file which is based on three levels of construction. The low-level is to build the system which states by defining all components used in the schematic diagram of the IPVTS such as mentioned in chapter 4. The medium-level states to define branches which is a component having two notified nodes such as inlet and outlet node, to able to connect all the objects together. And finally the high-level construction aims to define the plant loop and operation schemes necessary to run the simulation successfully. Each of the following levels will be discussed in this chapter with details.

## 5.2 System topology

At a first stage of the IPVTS plant loop simulation it is important to convert the schematic diagram to a plant loop Energy Plus diagram [24]. This diagram ease to model and connects all components together. The program uses branches to construct the loop. A Branch is a component having two nodes on both sides, more precisely an inlet and an outlet node. In Figure 5.3 the plant loop diagram is presented as per the external interface guidance [24].

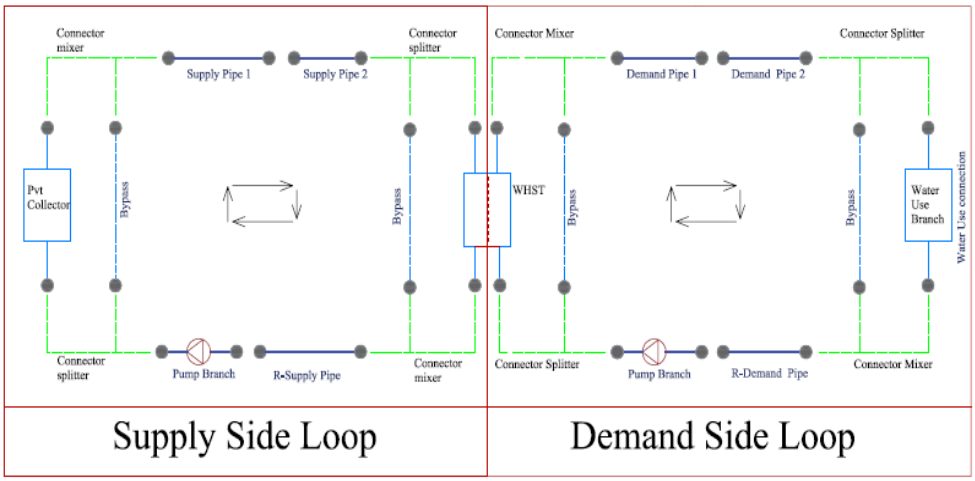


Figure 5.2: External interface supply and demand side of the plant loop

As it can be observed in this loop all the components are separated and connected via nodes, in terms to ease the modeling on IDF file by clarifying its connections, branches and node names for each of the components. The Supply side loop contains the collector, pipes, two variable speed pumps and the water heater stratified tank. For the demand side loop the use side outlet node of WHST is connected via pipes to a water use equipment and in case of there is no extraction the DHW is bypassed and returns to the use inlet node of WHST via a pump when extraction is not occurred. However, in Figure 5.4 all the nodes, branches connector splitters, connector mixers and components names are presented as modeled in EnergyPlus.

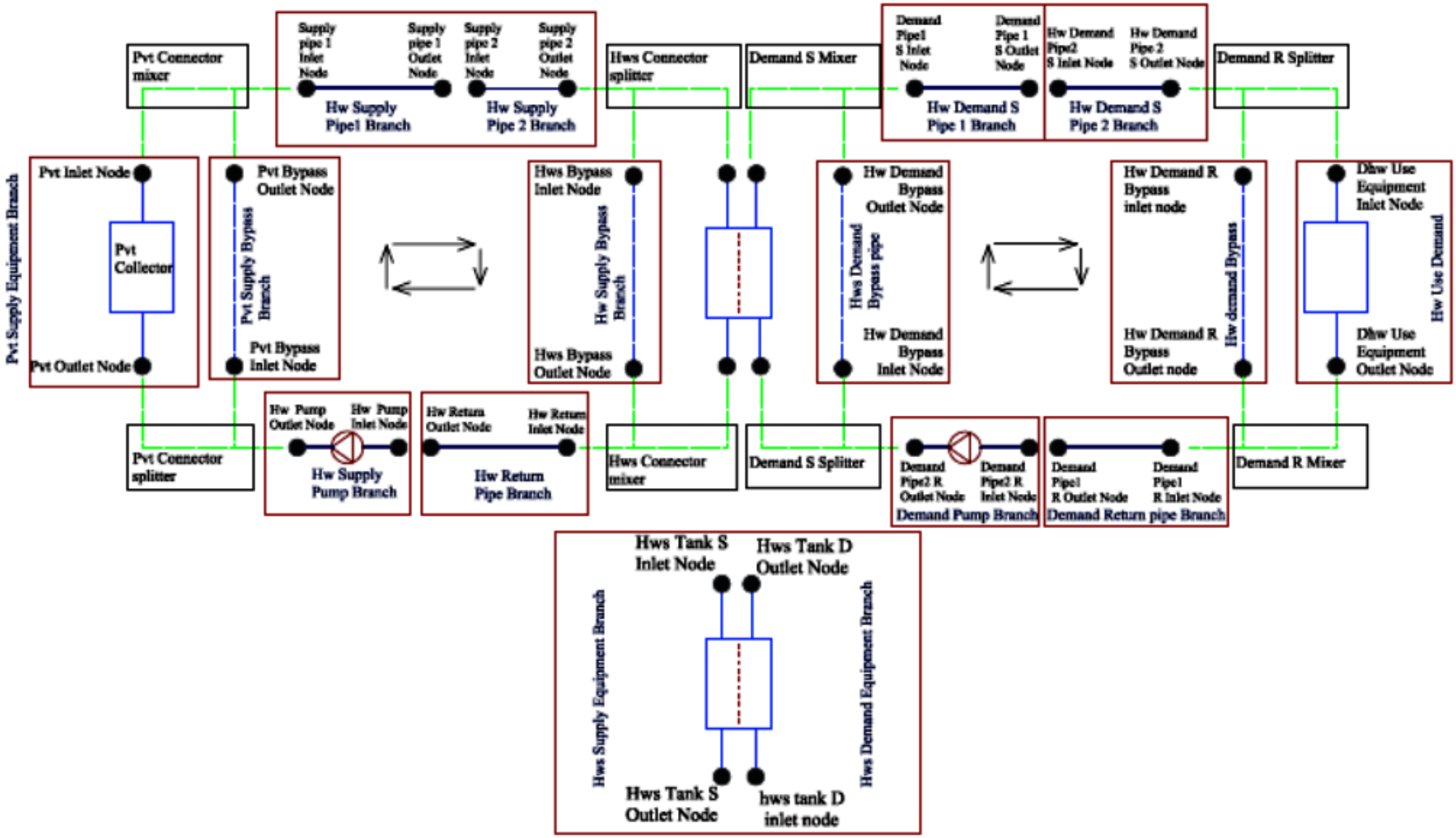


Figure 5.3: Plant loop diagram, with nodes, branches, components, and connector splitters and mixers name

## 5.3 Low-level plant construction

This level of construction consists of defining all the components using the objects found in the subheadings. Objects in the IDF file of the presented components will be used to identify inputs parameters. The Input/Output Ref. [25] explains the implementation of the input characteristics.

### 5.3.1 Water storage tank modeling

The water heater tanks are found on the IDF file as “Waterheater:stratified” Different aspect ratios has been selected for this object for different capacities which are 100L, 120L, 150L and 200L as discussed in chapter 3. The WHST sizes are selected having the same use and source flow rates of 0.16L/s for the same actual demand. The parameters selected to model this object are presented in table 5.1. Upon these selected inputs the water heater stratified tanks with different capacities has been modeled and simulated.

The WHST is divided into ten nodes of equal volume. Using numerical methods the energy balance equation on the nodes is solved simultaneously by the differential equations. This WHST contain two heating elements on the IDF file Selected to be MasterSlave as Heater 2 is the slave and Heater 1 is the master, at which one of them can be on at a time. For this study both heaters are selected to be off, there are no auxiliary heating.

As it is been informed for three schemes that characterizes tanks sizes, scheme one characterizations are going to be displayed in table 5.1. Scheme two and scheme three having the same tank size and capacity characteristics are represented in table 5.2.

Table 5.1: Water heater stratified tanks scheme 1 parameters.

| Parameter | Tank 100L | Tank 120L | Tank 150L | Tank 200L |
|---|---|---|---|---|
| Tank Volume | 0.10 $m^3$ | 0.12 $m^3$ | 0.15 $m^3$ | 0.20 $m^3$ |
| Tank Height | 0.96 m | 0.96 m | 0.98 m | 1.01 m |
| Tank Diameter | 0.36 m | 0.44 m | 0.44 m | 0.50 m |
| Use Side Flow rate | Autosize | Autosize | Autosize | Autosize |
| Source Side Flow rate | Autosize | Autosize | Autosize | Autosize |

Table 5.2: Water heater stratified tanks scheme 2a and 2b parameters.

| Parameter | Tank 100L | Tank 120L | Tank 150L | Tank 200L |
|---|---|---|---|---|
| Tank Volume | 0.10 $m^3$ | 0.12 $m^3$ | 0.15 $m^3$ | 0.20 $m^3$ |
| Tank Height | 0.83 m | 0.95 m | 1.19 m | 1.59 m |
| Tank Diameter | 0.40 m | 0.40 m | 0.40 m | 0.40 m |
| Use Side Flow rate | Autosize | Autosize | Autosize | Autosize |
| Source Side Flow rate | Autosize | Autosize | Autosize | Autosize |

### 5.3.2 Hybrid PV/T Collector modeling

The Hybrid PV/T solar collector object is found in the IDF file as "solarCollector:FlatPlate:PhotovoltaicThermal". The PV/T collector is connected to the plant loop, for the collection of thermal energy to be utilized. As per reference [25] identification, "the PVT collector is modeled as a hot water solar collector and the working fluid is selected to be water". The parameters selected to model the

collector are being presented in Table 5.3. These data inputs has been uploaded upon several other objects such as the performance, inverter, electrical load, photovoltaic generator and photovoltaic performance related to the modeling of PV/T thermal component.

Table 5.3: Photovoltaic Thermal collector parameters

| Parameter | Input | Unit |
|---|---|---|
| Thermal working fluid | Water | NA |
| Design flow rate | 0.00016 | $m^3/s$ |
| $f_a$ | 0.4 | Dimensionless |
| Thermal conversion efficiency | 0.40 | Dimensionless |
| Front surface emittance | 0.84 | Dimensionless |
| $f_a$ (solar cells) | 0.4 | Dimensionless |
| Value for cell efficiency | 0.12 | Dimensionless |

### 5.3.3 Pipe Connections

Components (WHST and PVT) are connected via pipes; such detail is not needed in EnergyPlus, where heat loss and pressure drop though pipes are not presented. Thus the object is used as a bypass and connection device only. However, a bypass branch is used to bypass the core operating components. This may ensure the circulation of the working fluid through the bypass pipe instead of components, in case when the operating components are not required. It should be noted that only one bypass per half loop is required [25].

### 5.3.4 Pump:VariableSpeed object

Based on the plant topology implication two variable speed pumps must be selected to complete the plant loop. Supply side loop pump is located at the return way of the PVT collector where water is being re-heated, such as the demand loop pump has been located at the return way of the storage tank. The following Table presents the parameters of both pumps.

Table 5.4: Variable speed pumps parameters.

| Parameters | Supply side pump | Demand side pump | Unit |
|---|---|---|---|
| Design maximum Flow rate | 0.00016 | 0.00016 | $m^3/s$ |
| Design pump head | 1 | 1 | Pa |
| Design minimum flow rate | Autosize | Autosize | $m^3/s$ |
| Pump control type | Intermittent | Intermittent | NA |

## 5.4 Medium-level plant construction

Upon the plant diagram presented in Figure 5.3 the objects branch, branchlist, nodelist, connector splitter, connector mixer and connector list has been filled in order to connect all components together. However, each component has at least two nodes and this may imply a branch is constructed. The branchlist simply provides the list of branches divided into four categories based on plant loop diagram, the plant is divided into supply and demand sides. Thus, these became supply system half loop, Demand system half loop, Supply usage half loop and demand usage half loop as shown in Figure 5.4. Branches and branchlist should be organized on the IDF file in flow order: inlet branch, the parallel branches (bypass pipes) then outlet branches [25].

The format statements of connector mixer and connector splitter input are similar. The connector splitter divides the circulation of water into two branches, the bypass pipe and the component. The connector mixer rejoins the divided water at the opposite side. Thus, it is remarkable that each half loop must have one connector splitter and one connector mixer. For the nodelist object all the nodes must be identified following the flow of water, this may afford to the program the overall connection to complete the level construction.

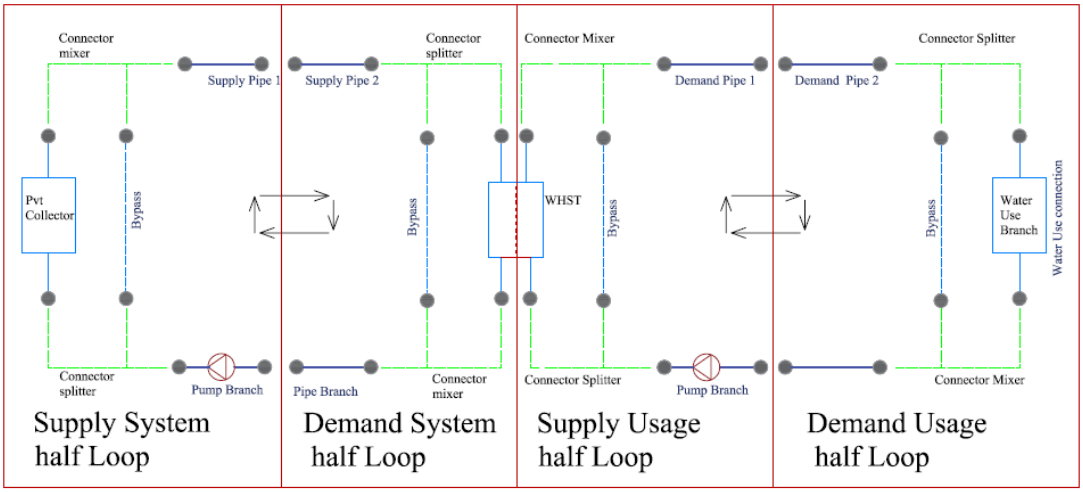


Figure 5.4: Showing the four categories of water heating plant loop

## 5.5 High-Level plant construction

This level requires to edit plant loop characteristics, the “PlantLoop” object inputs aims to identify the plant loop equipment. For this schematic there are two equipment such as the PVT collector and the WHST to be identified. The WHST plant equipment operation scheme is another object on the IDF file presented in Table 5.5.

The Maximum and minimum Loop Temperature range between 70 °C and 15 °C in terms of safety and preventing errors. However, the field Load Distribution Scheme is set to be Optimal in order to meet plant loop demand. Thus, an algorithm is selected in purpose to sequence the equipments operations. However, there are two demand plant loop calculations scenarios at which the SingleSetpoint is selected in the field Plant Loop Demand Calculation Scheme. The Setpoint manager set a setpoint value which is single to each node. Common Pipe and Pressure Type fields require no simulations.

Table 5.5:The plant equipment operation scheme

| Field | Plant demand | Plant supply | Units |
|---|---|---|---|
| Fluid type | Water | Water | NA |
| Maximum loop Temperature | 70 | 70 | °C |
| Minimum Loop ‘Temperature | 15 | 15 | °C |
| Maximum Loop flow rate | 0.16 | 0.16 | L/s |
| Minimum Loop flow rate | 0 | 0 | L/s |
| Plant side | WHST | PV/T module | NA |
| Plant side Branch | Usage supply | System supply | NA |
| Load distribution | OPTIMAL | OPTIMAL | NA |
| Plant loop demand calculation | Single setpoint | Single setpoint | NA |

# Chapter 6

# RESULTS AND DISCUSSION

## 6.1 PVT Collector Result

The collector delivers electrical and thermal energy by exploiting solar radiation. The electrical power output of the PVT and associated solar radiation values are shown in figure 6.1 for two typical winter design days (20th and 21st of February). The electrical power generation is dependent on the amount of solar radiation absorbed by the collector. The total tilted radiation and beam tilted radiation are also represented in this figure which shows the relation between solar radiation and electrical power generation by PVT. The highest output achieved is 221.78 W for these particular days.

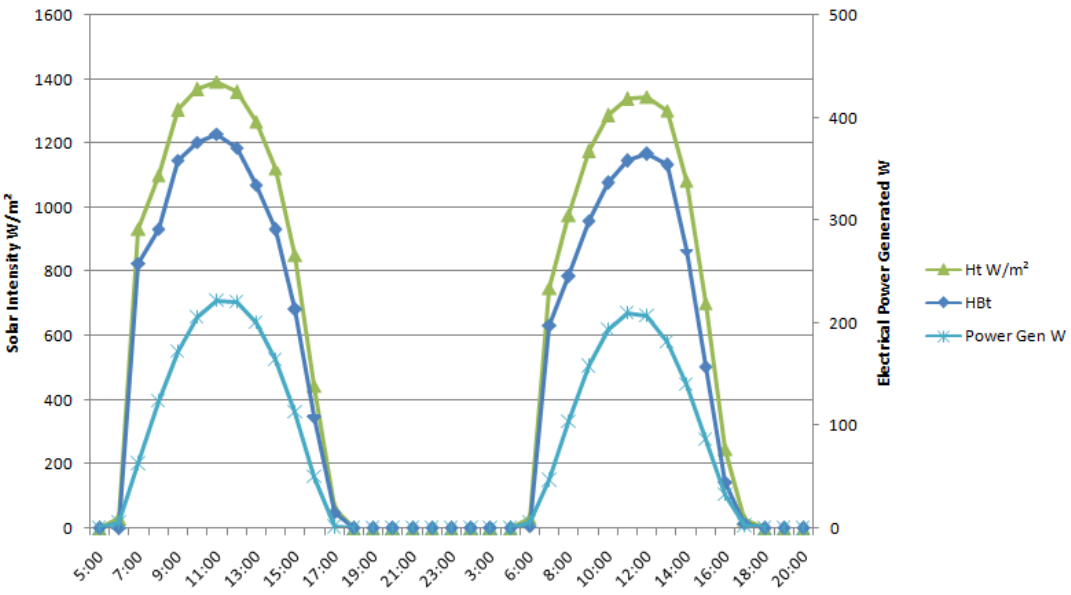


Figure 6.1: The Beam solar radiation on tilted surface and electrical power generated by PV/T module hourly (20th and 21st of February).

Solar radiation intercepted by the illuminated area of the PV/T collector is absorbed which allows converting it into electrical energy. The losses of energy conversion are released as heat and stored in the collector as thermal energy which increase the temperature of the photovoltaic panels. In the PVT system water is circulated through the system thus extracting the stored heat to water. This reduces the temperature of the PVT and increases the temperature of water.

The Unglazed PVT collector outlet node temperature is represented in figure 6.2 for scheme 1 and 2a and figure 6.3 for scheme 2b. The production of heat is dependent on the total solar radiation on the tilted surface. The temperature of the collector range between 50 °C to 15 °C. It is been observed a drop in temperature at the outlet node of the PVT collector during draw off periods.

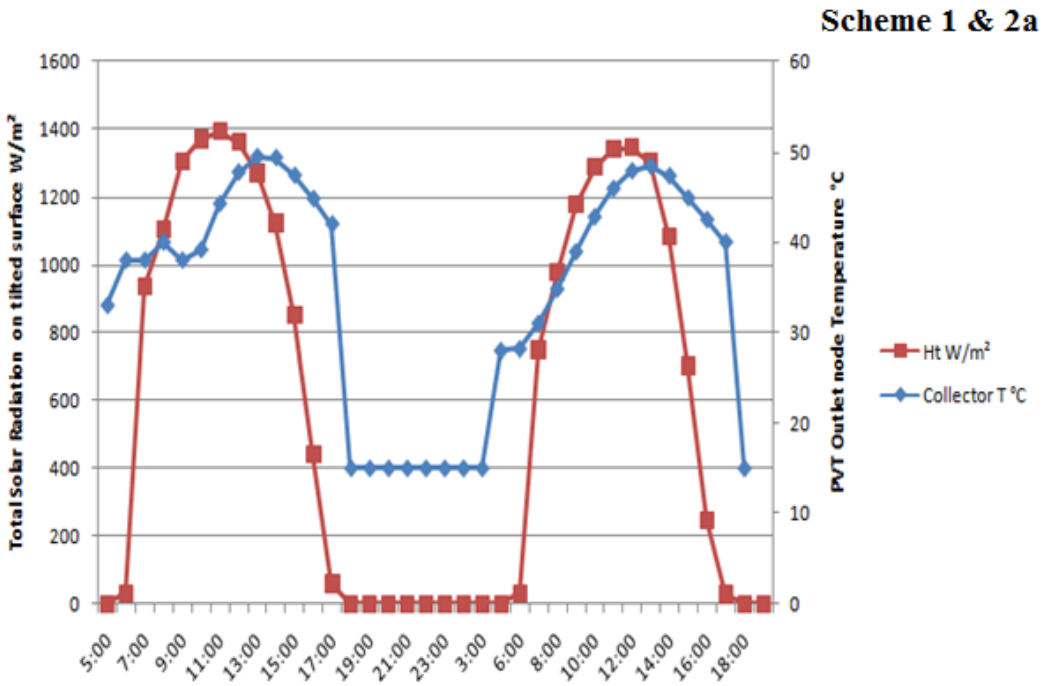


Figure 6.2: The total Solar radiation on tilted surface and Outlet temperature of the PVT collector for scheme 1 and 2a (20th and 21st of February).

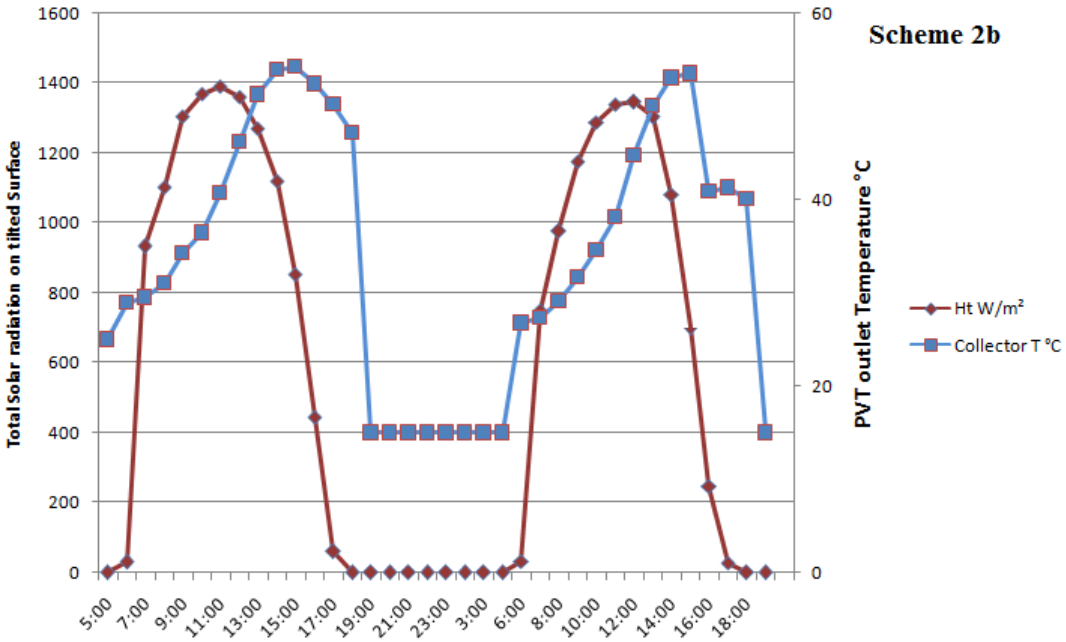


Figure 6.3: The total Solar radiation on tilted surface and Outlet temperature of the PVT collector for scheme 2b (20th and 21st of February).

## 6.2 Temperature profile of WHST

The temperature profile equation is given in chapter 3, the temperature of the water tanks ranges between 44.47 °C and 15 °C. This temperature is dependent on the node level, the extraction of hot water during draw off periods and mainly on the heat absorbed from the PV/T module when solar radiation is intercepted. The amount of water drawn from the tanks is the same during draw off periods. For scheme 1 and scheme 2a at each draw off period 576 L are extracted from the tank. For scheme 2b the draw off starts at the end of the day for a full extraction of DHW. The comparison between scheme 1 and scheme 2a enables us to understand how size of tanks can affect thermal stratification. However, for scheme 2a and scheme 2b the comparison will show how drawing water from the tank can affect the stratification inside the tank.

### 6.2.1 Temperature profile of 100 L tank

In Figure 6.4 (a) the transient temperature distribution inside the tank 100 L scheme 1 is displayed having a height of 0.96 m and diameter of 0.36 m, it can be observed that the curves are found to be at the highest z/H per T* which imply that thermal stratification was highly maintained through all times. The hot and cold water are separated properly and the thermocline region is found to be between node 2 and node 4 at 12:00 and 13:00, which imply that the thermocline region is well defined in the tank. The hot water temperature reached 42.53°C which is the target temperature as per Ref [3], [5] and [7] indicated.

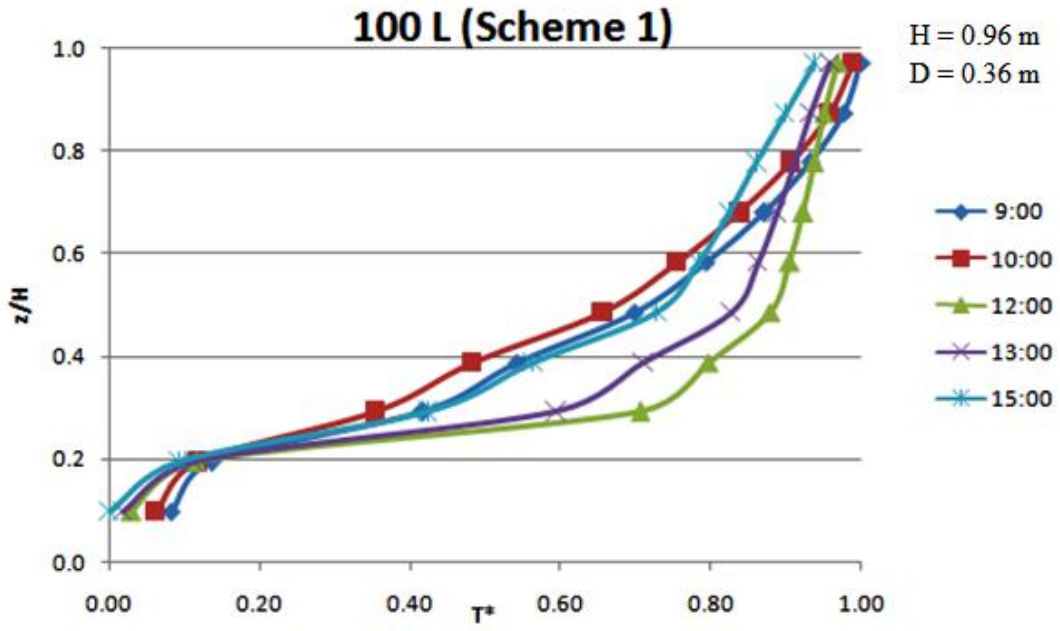


Figure 6.4 (a): Transient temperature distribution inside the 100 L tank scheme 1.

In Figure 6.4 (b) the 100 L tank scheme 2a has a higher diameter of 0.40 m and a lower height of 0.83 m compared with scheme 1, it is been observed that the temperature profile curves was slightly decreasing and distributed along the axis which imply that thermal stratification was unstable along the day. The maximum temperature achieved for this tank was 39.36 °C found in Table 6.1, which is also

lower compared with tank in scheme 1. For Figure 6.3 (c) the transient temperature distribution of 100 L tank scheme 2b is displayed at which the graph shows a similar performance of scheme 2a during day time. However, at 18:00 both tanks had the same temperature at this instant but at 21:00 for scheme 2a the temperature profile deceased to 0.78 as for scheme 2b the temperature profile is 0.5 which imply that hot water was fully extracted from the tank.

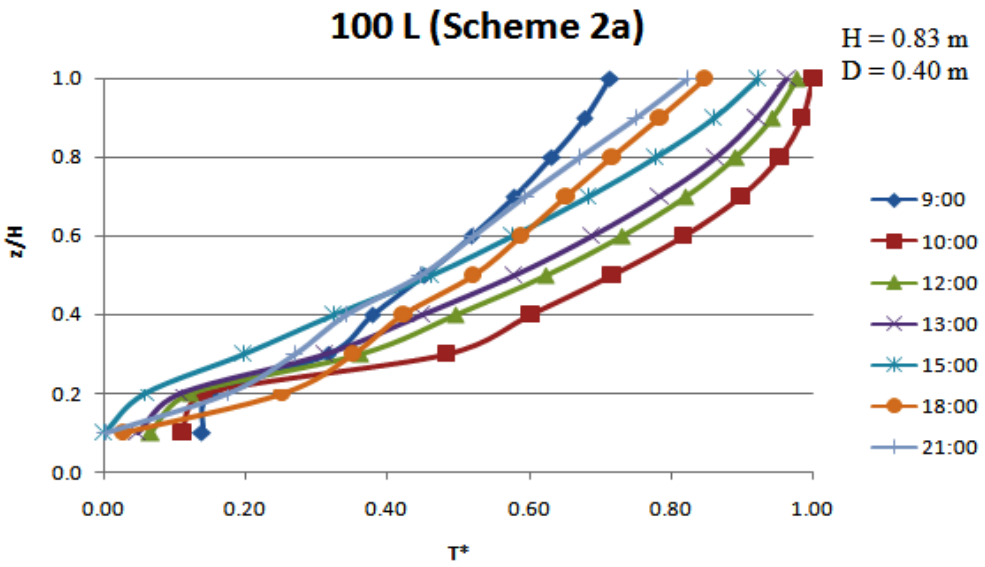


Figure 6.4 (b): Transient temperature distribution inside the 100 L tank scheme 2a.

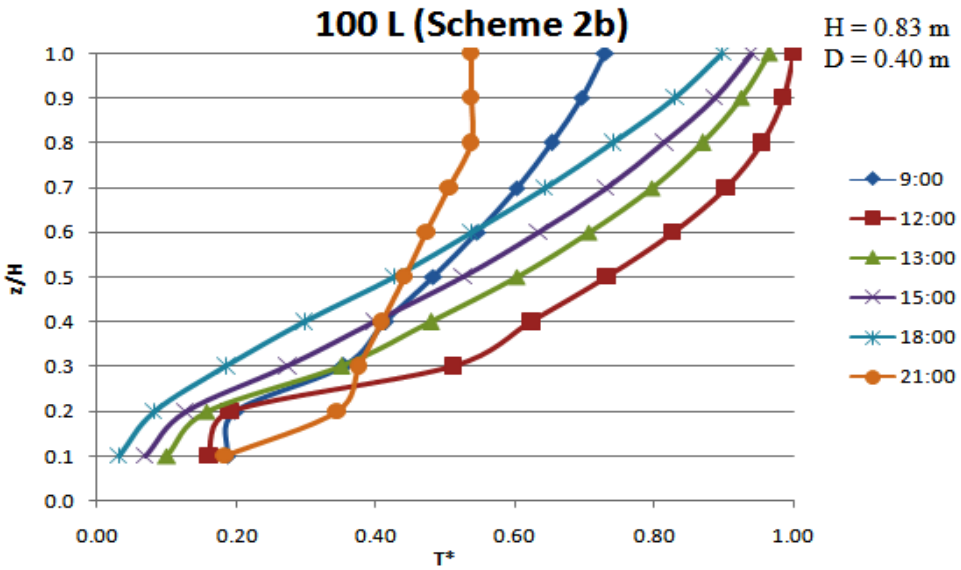


Figure 6.4 (c): Transient temperature distribution inside the 100 L tank scheme 2b.

Table 6.1: Water heater stratified tank 100 L results for all schemes.

| Parameter for 100L | Scheme1 | Scheme2a | Scheme2b |
|---|---|---|---|
| Height | 0.96 m | 0.83 m | 0.83 m |
| Diameter | 0.36 m | 0.40 m | 0.40 m |
| H/D | 2.07 | 2.66 | 2.66 |
| T max | 42.53 °C | 39.36 °C | 39.36 °C |

### 6.2.2 Temperature profile of 120 L tank

In Figure 6.5 (a), it can be observed that thermal stratification is degraded, at 9:00 and 10:00 when the first draw off starts the temperature profile was 0.5, as a reason of that the tank did not store hot water during morning hours (6:00 to 9:00). The hot water supplied to the tank during first draw off was fully extracted. At 12:00, 13:00 and 15:00 the thermocline region is found to be between node 2 and node 8 which imply that hot and cold water was highly mixed and thermal stratification was unstable. The highest temperature is found to be only at the top of the tank for 37.02 °C.

In Figure 6.5 (b) the transient temperature distribution of the tank 120 L scheme 2a is displayed with a height of 0.96 m and Diameter of 0.44 m, the graphs show a similar performance at 9:00 and 10:00 compared with scheme 1. However, for 12:00, 13:00 and 15:00 the thermal stratification improved compared with scheme 1, the thermocline region is found to be between node 2 and node 5 and the tank reached a maximum temperature of 37.02 °C. At 18:00 and 21:00 the temperature inside the tank decreased due to the absence of solar radiation.

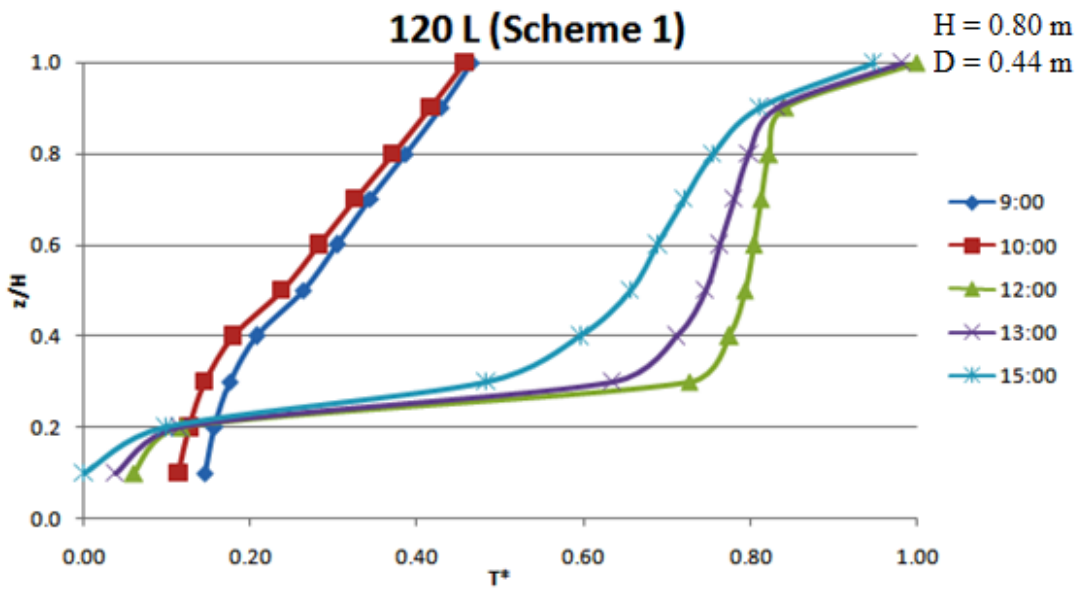


Figure 6.5 (a): Transient temperature distribution inside the 120 L tank scheme 1

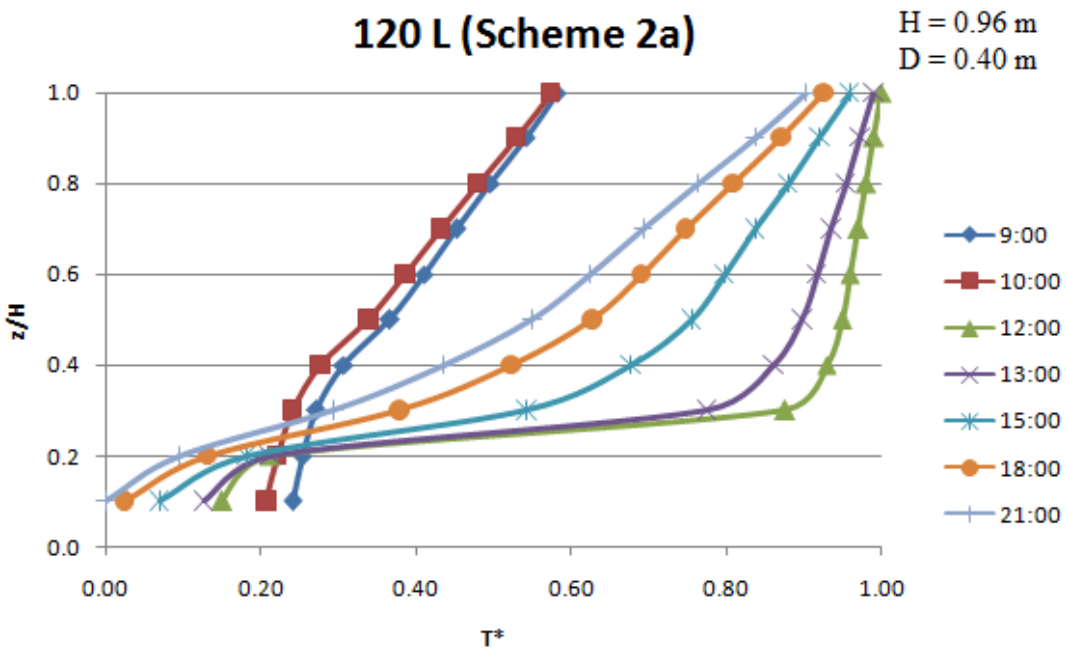


Figure 6.5 (b): Transient temperature distribution inside the 120 L tank scheme 2a.

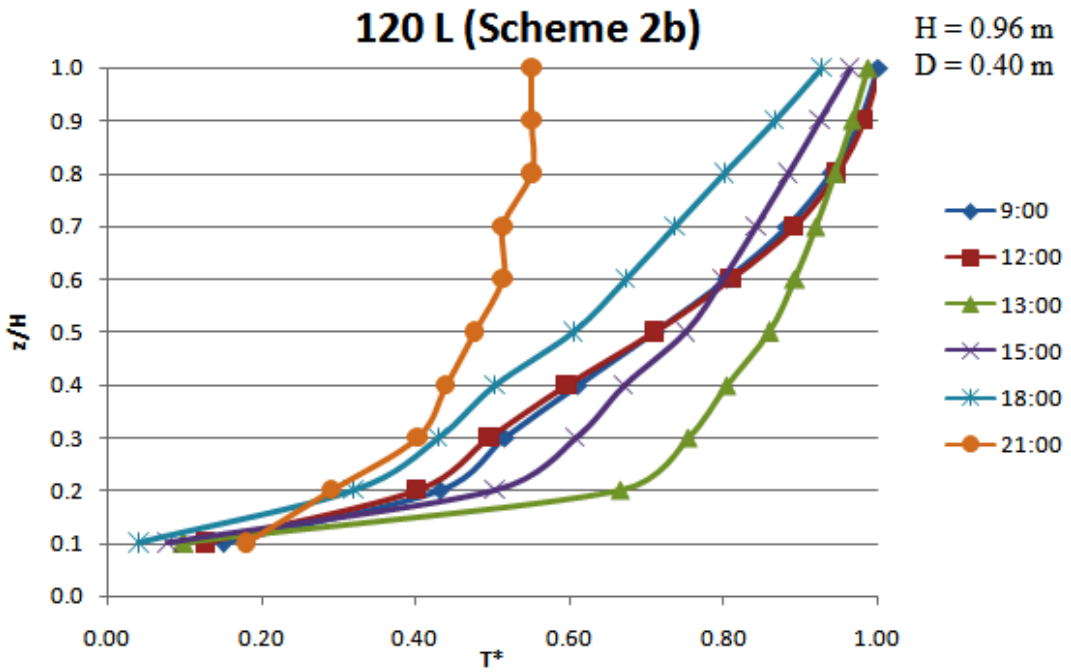


Figure 6.5 (c): Transient temperature distribution inside the 120 L tank scheme 2b

For the tank 100 L scheme 2b shown in Figure 6.5 (c) the temperature distribution inside the tank show a better performance and thermal stratification was maintained during all time compared with scheme 2a. As for at 18:00 the night draw off began and the curve at 21:00 show that hot water was fully extracted from the tank.

Table 6.2: Water heater stratified tank 120 L results for all schemes.

| Parameter for 120L | Scheme1 | Scheme2a | Scheme2b |
|---|---|---|---|
| Height | 0.80 m | 0.96 m | 0.96 m |
| Diameter | 0.44 m | 0.40 m | 0.40 m |
| H/D | 1.81 | 2.40 | 2.40 |
| T max | 37.02°C | 37.02°C | 37.22 °C |

### 6.2.3 Temperature profile of 150 L tank

In Figure 6.6(a) the transient temperature distribution inside the 150 L tank scheme 1 was displayed at which this tank has a height of 0.98 m and diameter of 0.44 m. As it can be observed that the temperature profile curves was slightly decreasing and distributed along the axis which imply that the thermal stratification for this tank was unstable during the day and the maximum temperature achieved for this tank is 37.62°C found in Table 6.1.

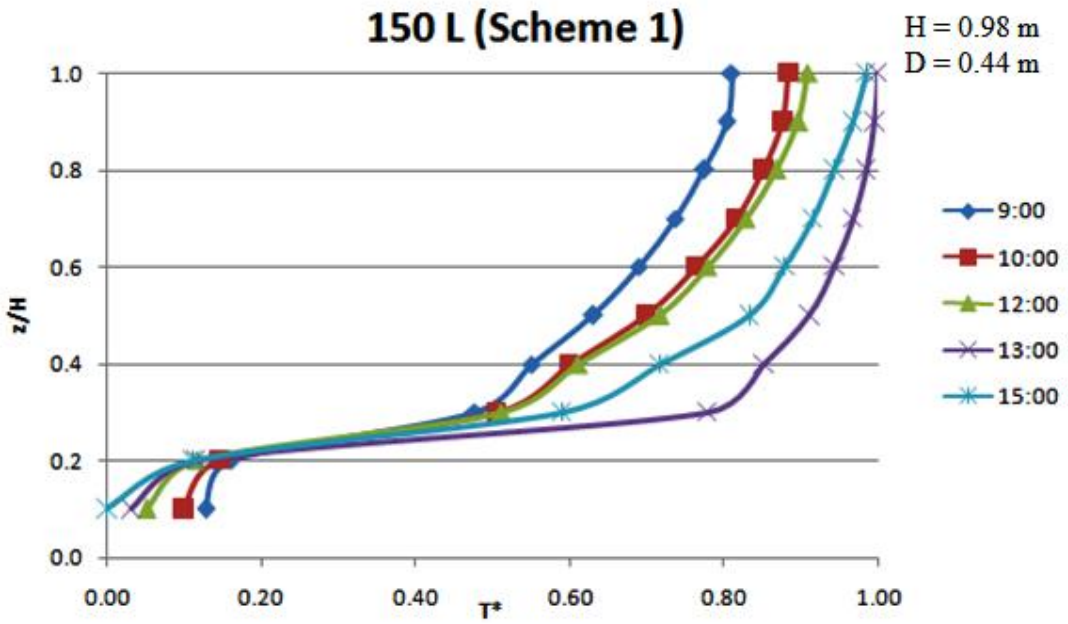


Figure 6.6 (a): Transient temperature distribution inside the 150 L tank scheme 1.

The temperature distribution inside the 150 L tank scheme 2a is displayed in Figure 6.6 (b), this tank has a higher height of 1.19 m and lower diameter of 0.40 m compared with tank of scheme 1. The curves in the graph are grouped to be between 0.8 and 1.0 of the temperature profile axis which imply that thermal stratification was highly maintained during all day and night hours. This tank shows a better performance than tank in scheme 1. As for the tank 150 L scheme 2b shown in Figure 6.6 (c) thermal stratification is highly maintained and slightly better than

scheme 2a due to the absence of hot water extraction during day hours. The first draw off in this scheme start at 18:00 and hot water was fully extracted as the curve at 21:00 show in the graph and the maximum temperature achieved was 37.22 °C shown in Table 6.3.

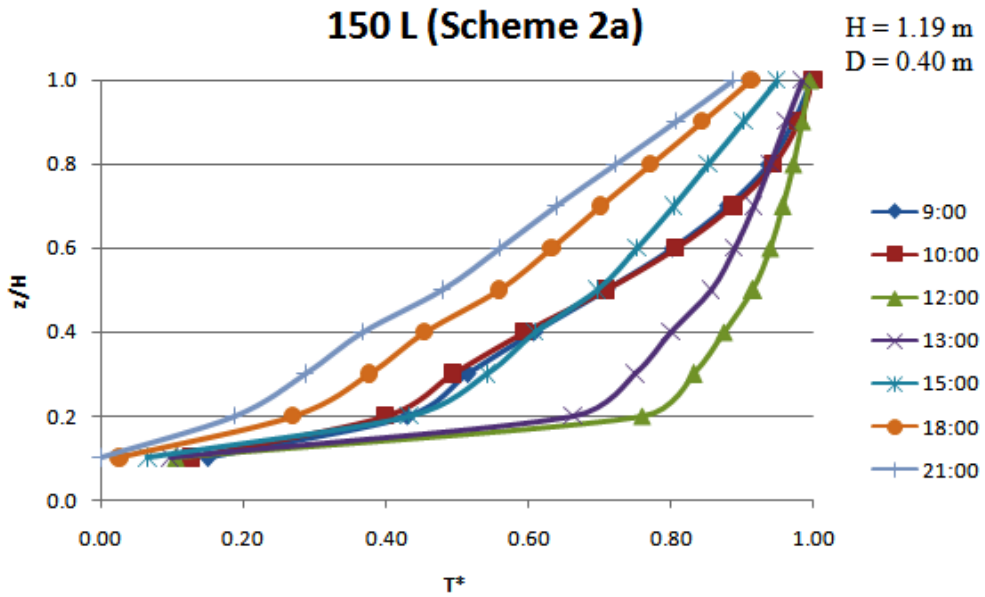


Figure 6.6 (b): Transient temperature distribution inside the 150 L tank scheme 2a

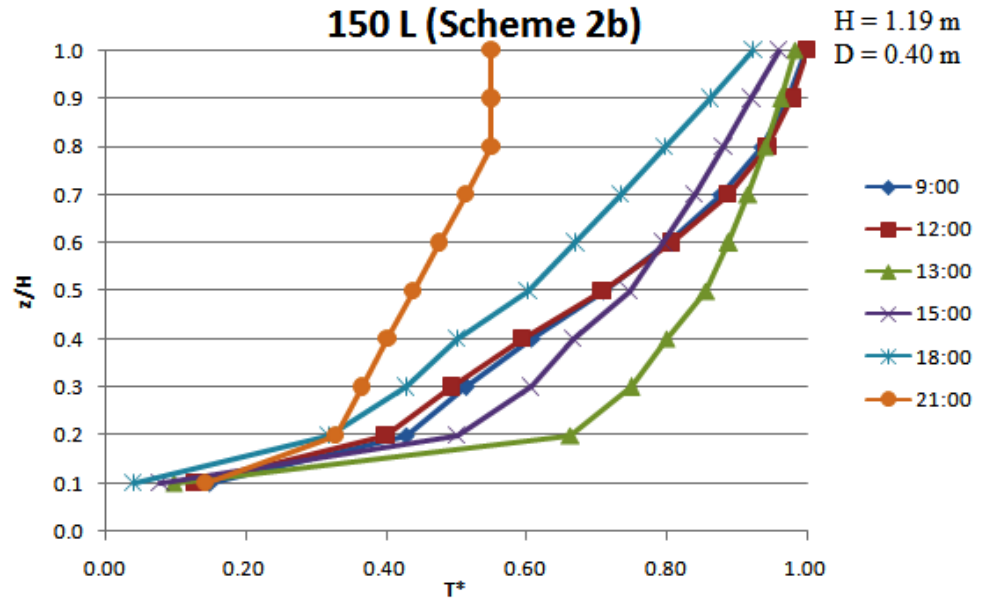


Figure 6.6 (c): Transient temperature distribution inside the 150 L tank scheme 2b

Table 6.3: Water heater stratified tank 150 L results for all schemes.

| Parameter for 150L | Scheme1 | Scheme 2b | Scheme2a |
|---|---|---|---|
| Height | 0.98 m | 1.19 m | 1.19 m |
| Diameter | 0.44 m | 0.40 m | 0.40 m |
| H/D | 2.22 | 2.97 | 2.97 |
| T max | 37.62°C | 37.22°C | 37.22 °C |

### 6.2.4 Temperature profile of 200 L tank

In Figure 6.7 (a) the transient temperature of the 200 L tank scheme 1 was displayed which has a height of 1.01 m and diameter of 0.50 m show that the curves in the graph at the highest node are found to be between 0.6 and 0.8 of the temperature profile axis along the day. Which imply that thermal stratification is not maintained and hot and cold water are highly mixed at which the highest temperature reached 37.16 °C as shown in Table 6.4.

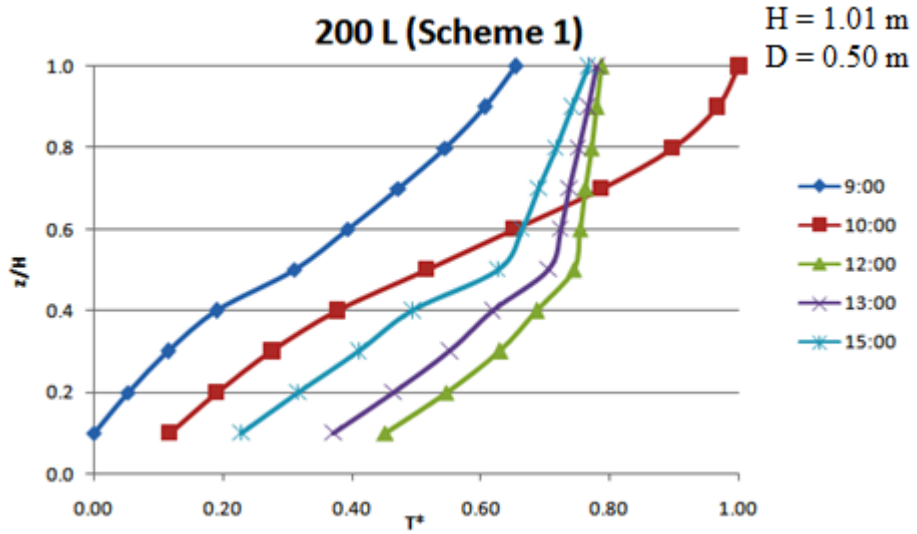


Figure 6.7 (a): Transient temperature distribution inside the 200 L tank scheme 1

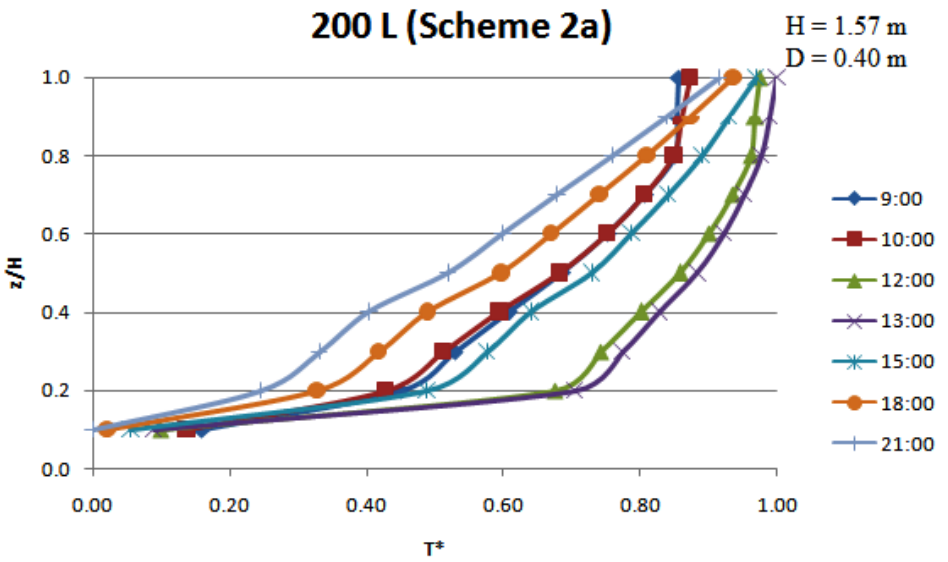


Figure 6.7 (b): Transient temperature distribution inside the 200 L tank scheme 2a

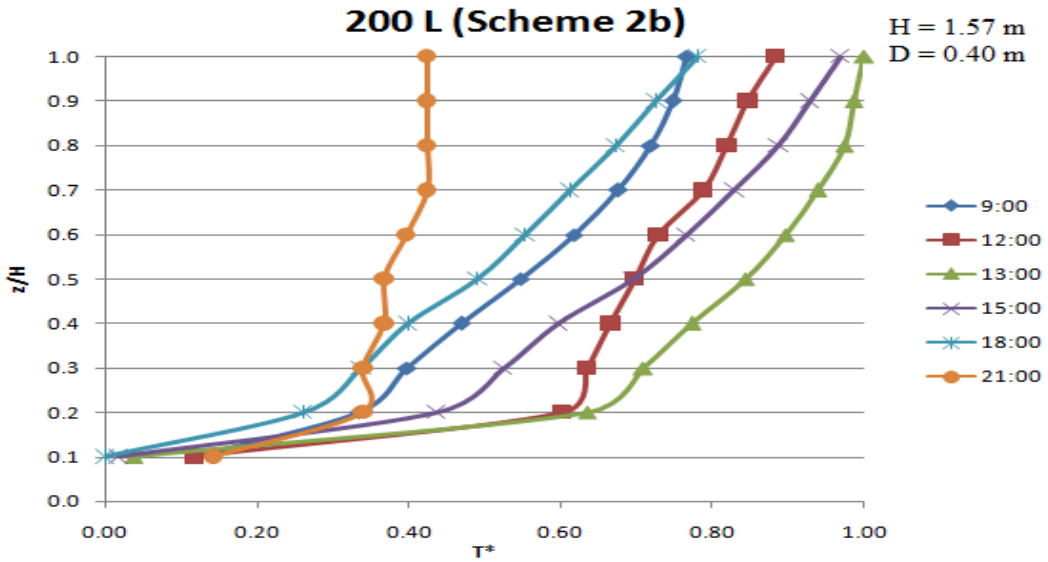


Figure 6.7 (c): Transient temperature distribution inside the 200 L tank scheme 2b

In Figure 6.7 (b) the temperature distribution inside the 200 L scheme 2a is displayed which has a higher height of 1.57 m and lower diameter of 0.40 m compared with scheme 1 tank. In this graph thermal stratification is highly maintained and has a better performance than scheme 1 tank. As it can be observed the curves at the highest node are located between 0.8 and 1.0 of the temperature profile axis. During

night time the hot water temperature start to decrease in the tank and the maximum temperature reached is 39.5 °C unless for the temperature of tank 200 L scheme 2b the maximum temperature was 44.46 °C shown in Table 6.4. the temperature distribution inside the tank 200 L scheme 2b represented in Figure 6.7 (c) show that thermal stratification was unstable and this due to heat losses to the ambient as a reason, the tank in scheme 2a the stratification was maintained but for a lower temperature than in scheme 2a as shown in Table 6.4. Such a case imply that the tank directly lose its temperature when solar radiation is decreased.

Table 6.4: Water heater stratified tank 200 L results for all schemes.

| Parameter for 200L | Scheme1 | Scheme2a | Scheme2b |
|---|---|---|---|
| Height | 1.10 m | 1.57 m | 1.57 m |
| Diameter | 0.48 m | 0.40 m | 0.40 m |
| T max | 37.16°C | 39.49°C | 44.46 °C |
| T max | 37.16°C | 39.49°C | 44.46 °C |

## 6.3 Heaters temperature distribution

The average temperature of the 100 L tank scheme 1 and scheme 2a are displayed in Figure 6.8. The tank of scheme 1 has an aspect ratio (H/D) of 2.66 which is higher than scheme 2a of 2.07, which showed a better performance as the tank reached a higher temperature of 33 °C compared to scheme 2a of 30 °C. It can be observed that the tank in scheme 1 stored hot water at an earlier time of the day compared with scheme 2a. During the first draw off the temperature of scheme 1 dropped to 29 °C and then the temperature increased to 34.5 °C. Both tank temperature collapse at the

end of the day due to absence in solar radiation, ambient losses and due to losses inside the tank as well, caused by internode conduction.

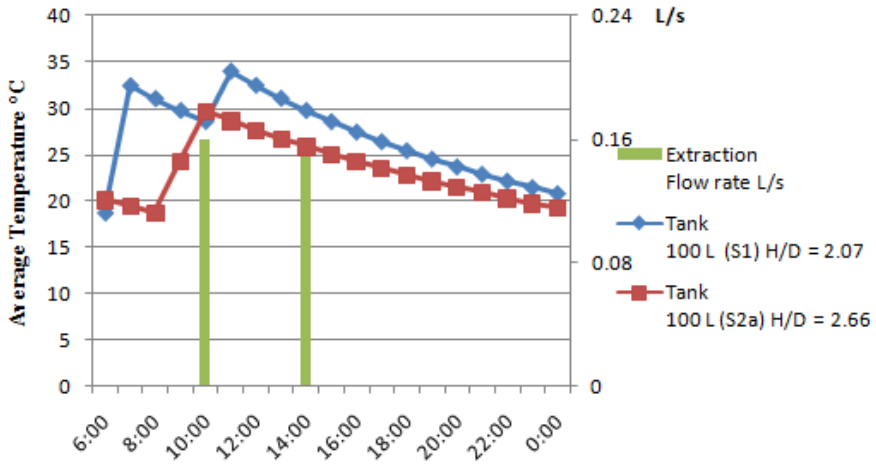


Figure 6.8: Average temperature of the 100 L tanks as a function of time for design day (21-February)

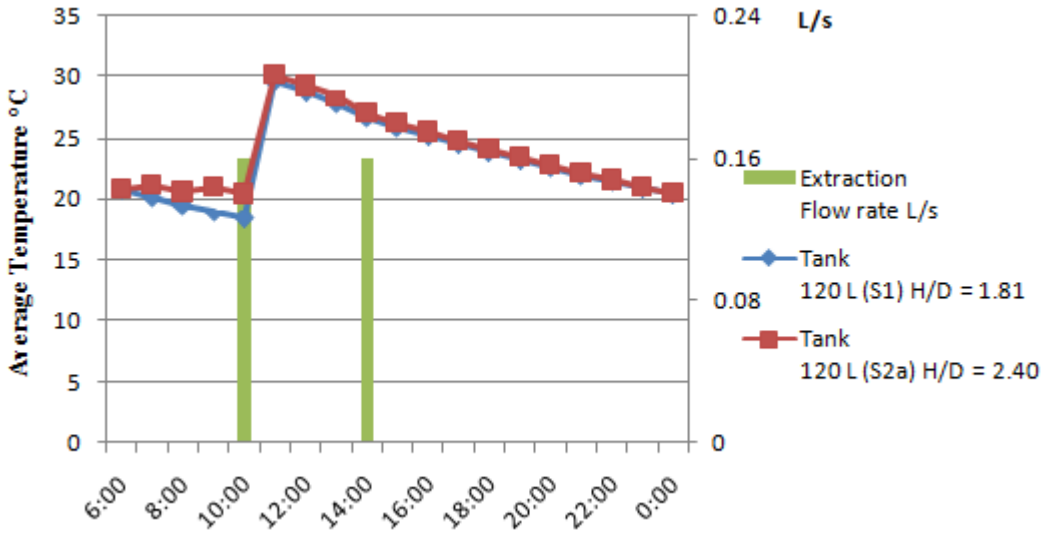


Figure 6.9: Average temperature of the 120 L tanks as a function of time for design day (21-February)

The average temperature of the 120 L tank scheme 1 and scheme 2a are displayed in Figure 6.9 the tank of scheme 1 has an aspect ratio (H/D) of 1.81 which is lower than scheme 2a of 2.40. The tank with a higher aspect ratio showed a slightly better performance during morning hours then the tank of scheme 2a. It can be observed

that the curves are almost similar but for scheme 2a the maximum temperature reached was 1.5 °C higher than for scheme 1. Both tank temperature collapse at the end of the day due to absence in solar radiation, due to ambient losses and due to losses inside the tank as well, caused by internode conduction.

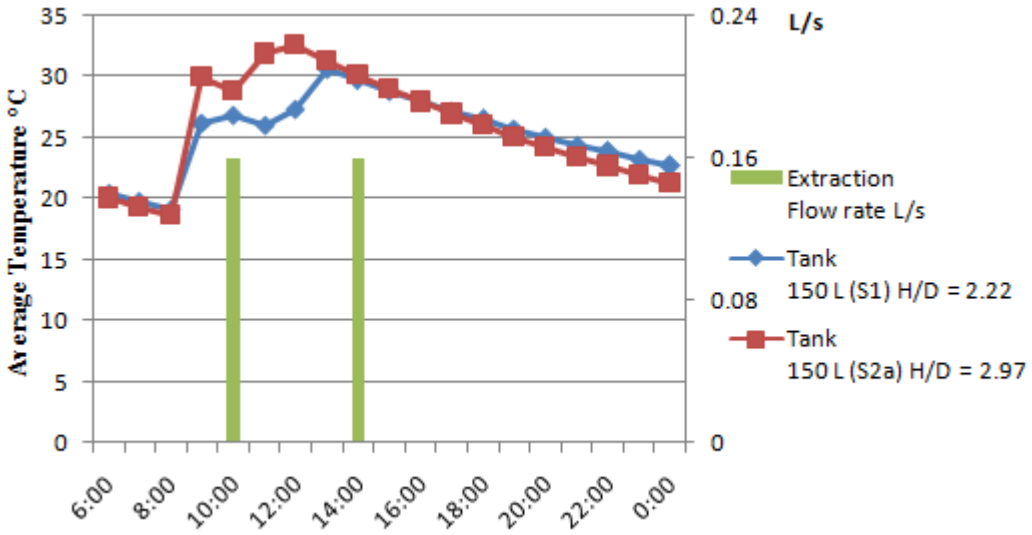


Figure 6.10: Average temperature of the 150 L tanks as a function of time for design day (21-February)

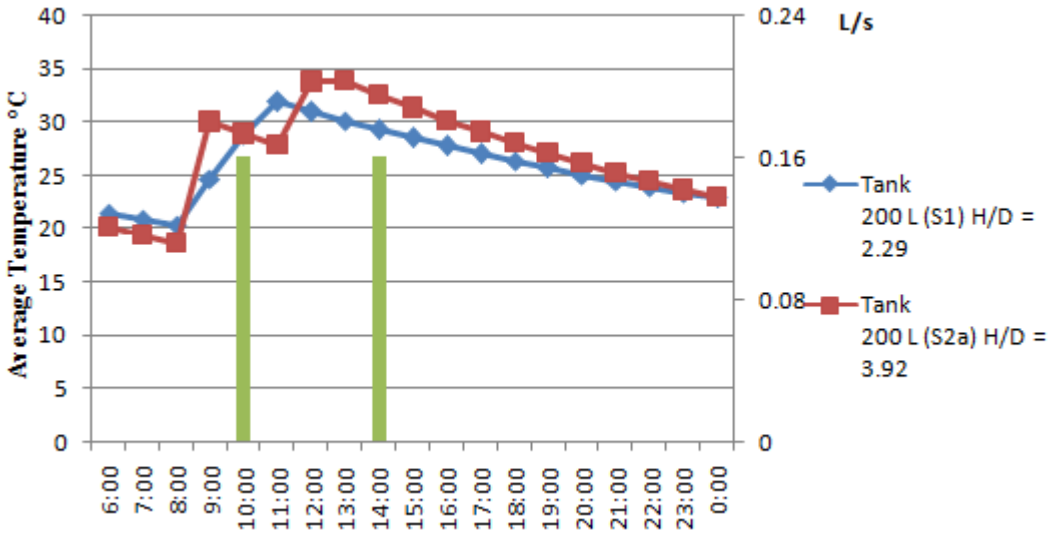


Figure 6.11: Average temperature of the 200 L tanks as a function of time for design day (21-February)

In Figure 6.10 the average temperature of the 150 L tank scheme 1 and scheme 2a are displayed. The tank of scheme 2a has an H/D of 2.97 which is higher than scheme 1 of 2.22, which showed a better performance as the tank reached a higher temperature of 33 °C compared to scheme 1 of 30 °C. It can be observed that the tank in scheme 2a stored hot water at an earlier time of the day compared to scheme 1. During the first draw off the average temperature of scheme 2a tank dropped to 29 °C as for scheme 2a the average temperature dropped to 26 °C. Both tank temperature collapse at the end of the day due to absence in solar radiation, ambient losses and due to losses inside the tank as well, caused by internode conduction.

The average temperature of the 200 L tank scheme 1 and scheme 2a are displayed in Figure 6.8. The tank of scheme 2a has an H/D of 3.92 which is higher than scheme 1 of 2.29. Scheme 2a tank showed a better performance as it required a higher temperature of 33 °C compared to scheme 1 of 31 °C. It can be observed that the tank in scheme 2a stored hot water at an earlier time of the day compared with scheme 2a. During the first draw off the temperature of scheme 1 dropped to 28 °C and then the temperature increased again to 33 °C. Both tank temperature collapse at the end of the day due to absence in solar radiation, ambient losses and due to losses inside the tank as well, caused by internode conduction.

# Chapter 7

## CONCLUSION AND FUTURE WORK

### 7.1 Storage tanks conclusion

In the present study an investigation was conducted on the temperature distribution effect for several tank sizes and capacities with different draw off periods. In order to explore the differences in temperature distribution inside the tanks for different H/D ratios. It is been realized that tanks with a higher H/D ratio results a better performance, as hot water is stored in the tank at an earlier time than of tanks with a lower H/D ratios. It can be observed also that tanks with a higher H/D ratios have a better stratification effect than tanks with a lower ratios shown in most Figures of Chapter 6.

Some similarities existed between the temperature profile curves of tank 150 L scheme 2a, tank 100 L scheme 1 and tank 200 L scheme 2a as stratification was intact and maintained. The temperature difference between the two tanks gave the ability to judge a suitable one, as for the 100 L the temperature reached 42.53°C, for 150 L the temperature was a bit lower for 37.62 °C and for tank 200 L temperature reached 44.46 °C. For 120 L tanks capacity it was observed that the thermocline region was steeper and stratification was unstable. It can be concluded that a higher H/D ratio should be considered for this capacity. Hence, it can be also concluded that the tank for 100 L capacity scheme 1 with H/D of 2.66 showed the best performance during two draw offs separated by 3 hours of standing time at which stratification

was highly maintained. And the optimum tank is found to be for 150 L scheme 2a with an H/D of 2.97 having a larger capacity of domestic hot water to be supplied. And finally tank with 200 L scheme 2a with an H/D of 3.92 showed a better performance than 150 L. The problem is that the hot water temperature of the 200 L tank directly decreases when solar radiation decrease due to the higher surface contact area with the environment which helps to decrease the temperature. The tank shall require a better insulation for conserving the heat inside and prevent any ambient losses.

## 7.2 Hybrid PV/T recommendation and future work

The system has critical points at which Temperature shall always be considered and scheduled. The Hybrid PV/T system overall efficiency increases when the module gets cooled Ref.[4][6][7]. Therefore, the fluid supplied to the module at the outlet node of the tank could have high temperature due to inversion mix as a main reason for this study. It should be also noted that in case of applying an electric or parasitic heater to the tank to cover thermal demands the same problem will be faced which it will even deteriorate the performance of the PV/T collector. Thus, a cold water Temperature at the inlet node of PV/T system will increase it is electrical efficiency, the module will last longer as bonds between silicon cells are always maintained and water is heated at the outlet node. Therefore, the circulating fluid must absorbs sufficient heat to cool panels as a main reason and to achieve hot water as a main purpose.

Solving this problem could be done by applying a thermostat at the outlet source node of the heater. The thermostat will control the temperature and keep it below 35 °C at least and actually the presence of a thermostat will complicates the system

more due to many connections and considerations. Therefore, in terms of simplicity the water supplied to the PV/T collector can be pumped directly from a cold water tank. The cold water then absorbs heat from the collector surface and dropped in the water tank. As a perspective work the Figure 7.1 a schematic diagram is represented to solve the problem, especially when the heater is applied to the system.

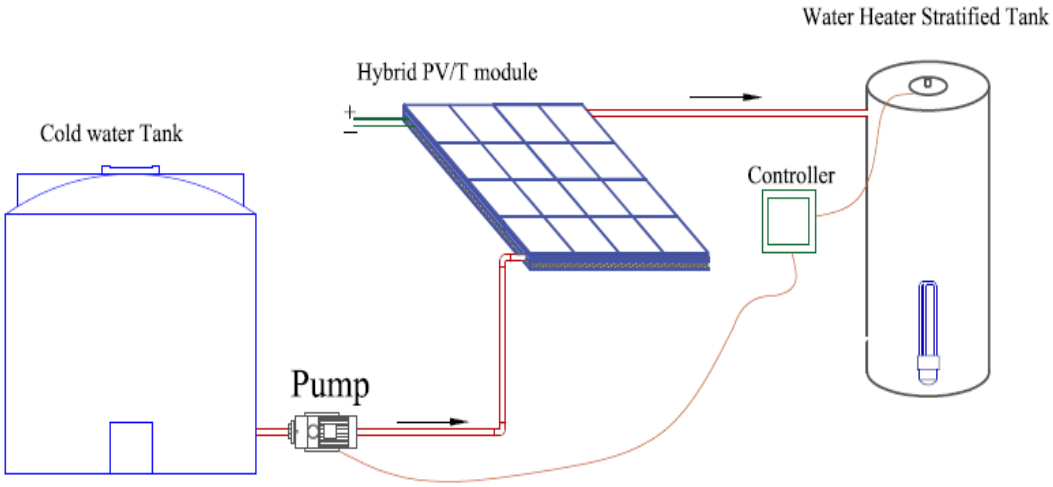


Figure 7.1: Schematic diagram for a PV/T system in service

# REFERENCES


[1] Gaynor, P.T., R.Y. Webb, and C.C. Lloyd. Low Enthalpy Heat Stirling Engine Based Electric Power Generation: A Research Design. *International Conference on Clean Electrical Power*. 2009. 615-618.

[2] Bergene, T., Vvik, O M. (1995). Model calculations on a flat-plate solar heat collector with integrated solar cells. *Solar energy*. 453-462.

[3] Kalogirou, S. A., Tripanagnostopoulos, Y. (2006). PV/T solar systems for domestic hot water and electricity production. *Energy Conversion and Management Journal*. 3368-3382.

[4] Hersch, P. Zweibel, K. (1982**).** Basic Photovoltaic Principles and Methods. Antimicrobial agents and chemotherapy Journal. 7250-7.

[5] Tripanagnostopoulos, Y., Souliotis, M., Battisti, R. Corrado, A. (2003). Application aspects of hybrid PV/T solar systems. ISES Solar World.

[6] Huang, Chao-yang Sung, Hsien-chao Yen, Kun-lung. (2012). Experimental Study of Photovoltaic/Thermal (PV/T) Hybrid System.

[7] Huang B.J, Lin T.H, Hung W.C, Sun F.S. (2001). Performance evaluation of solar photovoltaic/thermal systems. *Solar Energy*. 443-448.

[8] He W., Zhang Y., Ji J. (2011). Comparative experiment study on photovoltaic and thermal solar system under natural circulation of water. *Applied Thermal Engineering*. 3369-3376.

[9] Zhang X., Zhao X., Smith S., Xu J., Yu X. (2012). Review of R&D progress and practical application of the solar photovoltaic/thermal. (PV/T) technologies. *Renewable and Sustainable Energy Reviews*. 599-617.

[10] Chow T.T., He W., Ji J. (2006). Hybrid photovoltaic thermo syphon water heating system for residential application. *Solar Energy*. 298-306.

[11] Tripanagnostopoulos, Y., Souliotis, M., Battisti, R., Corrado, A. (2002). Application aspects of Hybrid PV/T solar system, 610 997472.

[12] Zuriyat Y.H. (1989). A Comparison Study of One-Dimensional Models for Stratified Thermal Storage Tanks.ASME Journal of Solar Energy. 205-210.

[13] Cynthia A.C., Stephen J.H. (2010). Heat Loss Characteristics for Typical Solar Domestic Hot Water Storage. Energy and Building. 1703-1710.

[14] Shyu R.J., Lin, J.Y., Fang, L.J. (1989). Thermal Analysis of Stratified Storage Tanks. ASME Journal of Solar Energy. 111, 54-61.

[15] Shahab A. (1999). An Experimental and Numerical Study of Thermal Stratification in a Horizontal Cylindrical Solar Storage Tank. Solar Energy. 409-421.

[16] Helwa, N.H., Mobarak, A.M., El-Sallak, M.S., El-Ghetany. (1996). Effect of Hot Water Consumption on Temperature Distribution in a Horizontal Solar Water Storage Tank.Applied Energy. 52, 185-197.

[17] Schwaner, T., Panggaard, M. (2015). Basics of thermal QCD. Specs Journal. 1-99.

[18] Afolayan, A.O. (2014). Effect of Tank Size on the Temperature Distributions for Solar Water Heaters. *Master thesis*. Gazimağusa, North Cyprus.pp.7, 9, 10, 11.

[19] ISISAN-Series 147. Sanitary plumbing systems. Istanbul; 1997 [in Turkish].

[20] Duffie, J.A., Beckman, W.A. (1991). Solar Energy Thermal Processes-Second Edition, Wiley-Interscience and Sons, New York.

[21] US Department of Energy http://apps1.eere.energy.gov/buildings/energyplus.

[22] Athinodoros, T. (2014). Performance assessment of building energy modeling programs and control optimization of thermally activated building systems, Master of Science Thesis, Faculty of Civil Engineering & Geosciences (CiTG).

[23] US Department of Energy. (2010). EnergyPlus Engineering Reference: The Reference to EnergyPlus Calculations. US Department of Energy. 1-847.

[24] US Department of Energy. (2015). External Interface(s) Application Guide. The Reference to EnergyPlus Application Guide. 4-5.

[25] US Department of Energy. (2014). Input Output Reference: The Encyclopedic Reference to EnergyPlus Input and Output. 1996-2015.

[26] Chen, C Julian. (2009). Physics of Solar Energy. Offered by Columbia Video Network. 2-6.